



# Functionally informed fine-mapping and polygenic localization of complex trait heritability

Omer Weissbrod<sup>1</sup>✉, Farhad Hormozdiari<sup>1</sup>, Christian Benner<sup>2</sup>, Ran Cui<sup>3</sup>, Jacob Ulirsch<sup>3,4</sup>, Steven Gazal<sup>1</sup>, Armin P. Schoech<sup>1</sup>, Bryce van de Geijn<sup>1</sup>, Yakir Reshef<sup>1</sup>, Carla Márquez-Luna<sup>5</sup>, Luke O'Connor<sup>3</sup>, Matti Pirinen<sup>2,6,7</sup>, Hilary K. Finucane<sup>3,8</sup> and Alkes L. Price<sup>1,3</sup>✉

**Fine-mapping aims to identify causal variants impacting complex traits. We propose PolyFun, a computationally scalable framework to improve fine-mapping accuracy by leveraging functional annotations across the entire genome—not just genome-wide-significant loci—to specify prior probabilities for fine-mapping methods such as SuSiE or FINEMAP. In simulations, PolyFun + SuSiE and PolyFun + FINEMAP were well calibrated and identified >20% more variants with a posterior causal probability >0.95 than identified in their nonfunctionally informed counterparts. In analyses of 49 UK Biobank traits (average  $n = 318,000$ ), PolyFun + SuSiE identified 3,025 fine-mapped variant-trait pairs with posterior causal probability >0.95, a >32% improvement versus SuSiE. We used posterior mean per-SNP heritabilities from PolyFun + SuSiE to perform polygenic localization, constructing minimal sets of common SNPs causally explaining 50% of common SNP heritability; these sets ranged in size from 28 (hair color) to 3,400 (height) to 2 million (number of children). In conclusion, PolyFun prioritizes variants for functional follow-up and provides insights into complex trait architectures.**

Genome-wide association studies (GWAS) of complex traits have been extremely successful in identifying loci harboring causal variants, but less successful in identifying the underlying causal variants, making the development of fine-mapping methods a key priority<sup>1,2</sup>. The power of fine-mapping methods<sup>3–12</sup> is limited due to strong linkage disequilibrium (LD), but it can be increased by prioritizing variants in functional annotations that are enriched for complex trait heritability<sup>7,8,10,13–17</sup>. However, previous functionally informed fine-mapping methods<sup>18–20</sup> have computational limitations and can use only genome-wide-significant loci to estimate functional enrichment (or can incorporate only a small number of functional annotations<sup>10</sup>), severely limiting the benefit of functional data.

We propose PolyFun, a computationally scalable framework for functionally informed fine-mapping that makes full use of genome-wide data by specifying prior causal probabilities for fine-mapping methods such as SuSiE<sup>21</sup> and FINEMAP<sup>22,23</sup>. PolyFun estimates functional enrichment using a broad set of coding, conserved, regulatory, minor allele frequency (MAF) and LD-related annotations from the baseline-LF model<sup>24–26</sup>.

We show in simulations with in-sample LD that PolyFun is well calibrated and more powerful than previous fine-mapping methods, with a >20% power increase over nonfunctionally informed fine-mapping methods. In simulations with mismatched reference LD, PolyFun remains well calibrated when reducing the maximum number of assumed causal SNPs per locus. We apply PolyFun to 49 complex traits from the UK Biobank<sup>27</sup> (average  $n = 318,000$ ) with in-sample LD and identify 3,025 fine-mapped variant-trait pairs with posterior causal probability >0.95, spanning 2,225

unique variants. Of these variants, 223 were fine-mapped for multiple genetically uncorrelated traits, indicating pervasive pleiotropy. We further used the posterior mean per-SNP heritabilities from PolyFun + SuSiE to perform polygenic localization, finding sets of common SNPs causally explaining 50% of common SNP heritability that range in size across many orders of magnitude, from dozens to millions of SNPs.

## Results

**Overview of methods.** PolyFun prioritizes variants in enriched functional annotations by specifying prior causal probabilities in proportion to predicted per-SNP heritabilities and providing them as input to fine-mapping methods such as SuSiE<sup>21</sup> and FINEMAP<sup>22,23</sup>. For each target locus, PolyFun robustly specifies prior causal probabilities for all SNPs on the corresponding odd (respectively even) target chromosome by: (1) estimating functional enrichments for a broad set of coding, conserved, regulatory and LD-related annotations from the baseline-LF 2.2.UKB model<sup>25</sup> (187 annotations; Methods and Supplementary Table 1) using an L2-regularized extension of S-LDSC<sup>17</sup>, restricted to even (respectively odd) chromosomes; (2) estimating per-SNP heritabilities for SNPs on odd (respectively even) chromosomes using the functional enrichment estimates from step 1; (3) partitioning all SNPs into 20 bins of similar estimated per-SNP heritabilities from step 2; (4) re-estimating per-SNP heritabilities for all SNPs on the target chromosome by applying S-LDSC to the 20 bins, restricted to odd (respectively even) chromosomes excluding the target chromosome; and (5) setting prior causal probabilities for SNPs on the target chromosome proportional to per-SNP heritabilities from step 4.

<sup>1</sup>Department of Epidemiology, Harvard T.H. Chan School of Public Health, Boston, MA, USA. <sup>2</sup>Institute for Molecular Medicine Finland (FIMM), University of Helsinki, Helsinki, Finland. <sup>3</sup>Program in Medical and Population Genetics, Broad Institute of MIT and Harvard, Cambridge, MA, USA. <sup>4</sup>Program in Biological and Biomedical Sciences, Harvard Medical School, Cambridge, MA, USA. <sup>5</sup>The Charles Bronfman Institute for Personalized Medicine, Icahn School of Medicine at Mount Sinai, New York, NY, USA. <sup>6</sup>Department of Public Health, University of Helsinki, Helsinki, Finland. <sup>7</sup>Department of Mathematics and Statistics, University of Helsinki, Helsinki, Finland. <sup>8</sup>Department of Medicine, Massachusetts General Hospital, Boston, MA, USA. ✉e-mail: [oweissbrod@hsph.harvard.edu](mailto:oweissbrod@hsph.harvard.edu); [aprice@hsph.harvard.edu](mailto:aprice@hsph.harvard.edu)

**Table 1 | Summary of methods evaluated in main simulations**

Method	Functional data	Max. no. of annotations	Max. no. of causal SNPs	Reference
fastPAINTOR–	No	N/A	Unlimited	19
fastPAINTOR	Yes	10	Unlimited	19
CAVIARBF1–	No	N/A	1	6
CAVIARBF1	Yes	Unlimited	1	20
CAVIARBF2–	No	N/A	2	6
CAVIARBF2	Yes	Unlimited	2	20
FINEMAP	No	N/A	10	22,23
PolyFun + FINEMAP	Yes	Unlimited	10	This article
SuSiE	No	N/A	10	21
PolyFun + SuSiE	Yes	Unlimited	10	This article

For each method we report whether it incorporates functional data, the maximum number of functional annotations that we specified under default simulation settings (for fastPAINTOR we selected the number of annotations that maximized power while maintaining correct calibration; Methods), the maximum number of causal SNPs modeled per locus (or the exact number for SuSiE and PolyFun + SuSiE), and the corresponding reference. For fastPAINTOR and CAVIARBF, – denotes the exclusion of functional data. For CAVIARBF, 1 or 2 denotes the maximum number of causal variants. PolyFun + FINEMAP uses a new version of FINEMAP introduced here that incorporates prior causal probabilities. N/A, not available.

The L2 regularization in step 1 improves the accuracy of per-SNP heritability estimation. The partitioning into odd and even chromosomes in steps 1 and 2, and the exclusion of the target chromosome in step 4 prevent winner's curse. The re-estimation of per-SNP heritabilities in step 4 ensures robustness to model misspecification.

PolyFun specifies prior causal probabilities in proportion to per-SNP heritability estimates:

$$P(\beta_i \neq 0 | \mathbf{a}_i) \propto \text{var}[\beta_i | \mathbf{a}_i], \quad (1)$$

where  $\beta_i$  is the causal effect size of SNP  $i$  in standardized units (the number of s.d. increases in phenotype per 1 s.d. increase in genotype),  $\mathbf{a}_i$  is the vector of functional annotations of SNP  $i$  and  $\text{var}[\beta_i | \mathbf{a}_i]$  is the estimated per-SNP heritability of SNP  $i$  from step 4 (Methods).

A key distinction between PolyFun and previous functionally informed fine-mapping methods<sup>10,18–20</sup> is the use of the entire genome and a large number of functional annotations to estimate prior causal probabilities. We exploited the computational scalability of PolyFun (together with SuSiE<sup>21</sup>) to fine-map up to 2,763 overlapping 3-Mb loci spanning the entire genome (Methods). We subsequently used our fine-mapping results to perform polygenic localization, identifying minimal sets of common SNPs causally explaining a given proportion of common SNP heritability. Details of the PolyFun method are provided in Methods; we have released open-source software implementing PolyFun together with SuSiE<sup>21</sup> and FINEMAP<sup>22</sup>. In all main simulations and analyses of real traits, we applied PolyFun using summary LD information estimated directly from the target samples (for running both S-LDSC and SuSiE or FINEMAP), as previously recommended for fine-mapping methods<sup>12,28</sup>.

**Main simulations.** We evaluated PolyFun via simulations using real genotypes from 337,491 unrelated UK Biobank British samples<sup>27</sup>. We analyzed 10 3-Mb loci on chromosome 1, each containing 1,468–27,784 imputed SNPs with MAF  $\geq 0.001$  and INFO score  $\geq 0.6$  (including short indels; Supplementary Table 2). We estimated prior causal probabilities using 18,212,157 genome-wide imputed SNPs with MAF  $\geq 0.001$  and INFO score  $\geq 0.6$ . We simulated traits with heritability equal to 25% and a genome-wide proportion of causal SNPs equal to 0.5%, with each target locus including 10 causal SNPs jointly explaining heritability of 0.05%. We specified prior causal probabilities using the baseline-LF model<sup>25</sup> with meta-analyzed functional enrichments from real data analyses (Supplementary Table 3). We generated summary statistics using  $n = 320,000$  samples. Further details are provided in Methods.

We evaluated ten fine-mapping methods (Methods and Table 1). We assessed calibration via the proportion of false positives among SNPs with posterior causal probability (posterior inclusion probability (PIP)) above a given threshold (for example, PIP  $> 0.95$ ), aggregating the results across all simulations; we refer to this quantity as the false discovery rate (FDR). For each PIP threshold, we estimated the FDR as the 1 – PIP threshold, which is more conservative than an exact estimate (Fig. 1a,b, Supplementary Note and Supplementary Table 4). No method except CAVIARBF2– and CAVIARBF2 had significantly inflated FDRs, although fastPAINTOR and CAVIARBF1 had suggestive evidence of inflated FDRs. We assessed power via the proportion of true causal SNPs with a PIP above a given threshold, aggregating the results across all simulations. PolyFun + FINEMAP was the most powerful method, identifying  $> 5\%$  more causal SNPs with a PIP  $> 0.95$  than PolyFun + SuSiE and  $> 20\%$  more causal SNPs with a PIP  $> 0.95$  than FINEMAP; PolyFun + SuSiE was the second most powerful method, identifying  $> 25\%$  more causal SNPs with a PIP  $> 0.95$  than SuSiE (Fig. 1c,d and Supplementary Table 4). These results demonstrate the benefits of prioritizing SNPs using functional annotations.

We evaluated the computational cost of each method. SuSiE and PolyFun + SuSiE were much faster than each other methods, fine-mapping a 3-Mb locus in 5 min on average (excluding fixed preprocessing time; see below) (Fig. 1e and Supplementary Table 4). CAVIARBF methods allowing more than two causal SNPs per locus were not evaluated, owing to prohibitively slow computation time. PolyFun also requires fixed preprocessing time (steps 1–4; see Overview of methods) of 630 min on average; when restricting analyses to subsets of loci, PolyFun + SuSiE was still faster than all other functionally informed methods when analyzing  $> 23$  loci (Fig. 1f).

We performed additional experiments to assess the robustness of PolyFun to model misspecification of functional architectures, to assess the individual impact of each of steps 1–5 of PolyFun on fine-mapping performance and to explore additional simulation settings (Supplementary Note, Extended Data Figs. 1–5 and Supplementary Tables 4–6).

We conclude from these experiments that PolyFun + FINEMAP and PolyFun + SuSiE outperformed all other methods, with a 3.4× faster runtime for the latter. Thus, we restricted our analyses in the remainder of this article to SuSiE and PolyFun + SuSiE.

**Simulations with mismatched reference LD.** Our main simulations used in-sample LD computed directly from the target samples. Although we have publicly released summary LD information

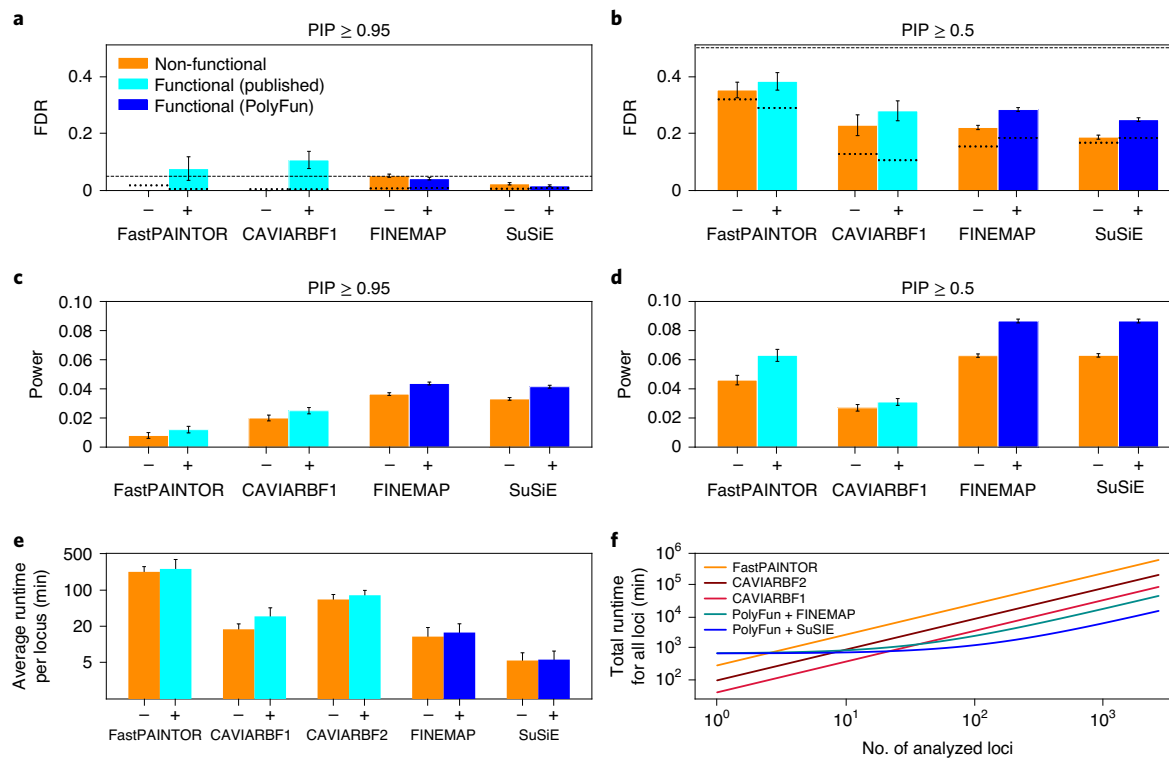


**Fig. 1 | Calibration, power and computational cost of fine-mapping methods in main simulations.** **a,b**, FDR at  $PIP = 0.95$  (**a**) and  $PIP = 0.5$  (**b**). Upper dashed horizontal lines denote conservative FDR estimates. Lower dotted horizontal lines denote anti-conservative FDR estimates, which are not recommended (Supplementary Note). **c,d**, Power at  $PIP = 0.95$  (**c**) and  $PIP = 0.5$  (**d**). The first bar of each method uses nonfunctionally informed fine-mapping (denoted as  $-$ ) and the second uses functionally informed fine-mapping (denoted as  $+$ ). **e**, The average runtime required to fine-map a 3-Mb locus in a genome-wide analysis (log scale). The first bar of each method uses nonfunctionally informed fine-mapping (denoted as  $-$ ) and the second uses functionally informed fine-mapping (denoted as  $+$ ). **f**, The total runtime required to fine-map different numbers of loci, for functionally informed fine-mapping methods only (log scale). The runtimes of PolyFun + SuSiE and PolyFun + FINEMAP are sublinear because they include the fixed preprocessing cost of computing prior causal probabilities (630 min). Error bars denote the s.e. Numerical results, including results for CAVIARBF2– and CAVIARBF2, and the results in **f** for nonfunctionally informed methods, are reported in Supplementary Table 4.

for British-ancestry UK Biobank samples as part of the present study, there are many settings in which researchers conducting fine-mapping cannot obtain in-sample LD, and instead use LD information from an external LD reference panel<sup>29</sup>. We performed extensive simulations to assess how fine-mapping performance is impacted by LD mismatch between the target sample and the LD reference panel. We specifically considered: (1) nonoverlapping target and reference samples; (2) sample sizes of the target sample and reference panel; (3) differences in ancestry; (4) presence of related individuals in the target sample; and (5) SNPs available for analysis in the target sample and reference panel.

We performed 19 experiments, described in detail in Table 2, the Supplementary Note and Supplementary Table 7. We quantified how mismatched reference LD impacts fine-mapping performance via the maximum number of assumed causal SNPs per locus (denoted as  $L$ ) which maintains  $FDR < 0.05$  at a  $PIP = 0.95$  threshold. Based on these experiments we provide fine-mapping best-practice recommendations: (1) PolyFun + SuSiE should ideally use in-sample LD from the GWAS target sample, with  $L = 10$ ; (2) PolyFun + SuSiE can alternatively use a nonoverlapping LD reference panel from the target population spanning  $\geq 10\%$  of the target sample size, with  $L = 10$ ; (3), PolyFun + SuSiE can be used without an LD reference panel by specifying  $L = 1$ ; we caution that use of an LD reference panel with even subtle population differences with  $L > 1$  may lead to false-positive results; (4) PolyFun + SuSiE can be used in the presence of related individuals in the target sample (but these results apply to the typical levels of relatedness observed in

the UK Biobank); and (5) PolyFun + SuSiE should include as many well-imputed SNPs from the target locus as possible to minimize the risk of omitting causal SNPs. The real-world implications of these best-practice recommendations are dealt with in the Discussion.

**Functionally informed fine-mapping of 49 complex traits.** We applied PolyFun + SuSiE to fine-map 49 traits in the UK Biobank, including 33 traits analyzed in refs. <sup>30,31</sup>, 9 blood cell traits analyzed in ref. <sup>12</sup> and 7 metabolic traits (average  $n = 318,000$ ; Supplementary Table 8). For each trait we fine-mapped up to 2,763 overlapping 3-Mb loci spanning 18,212,157 imputed SNPs with  $MAF \geq 0.001$  and INFO score  $\geq 0.6$  (including short indels; excluding three long-range LD regions and loci with close to zero heritability; Methods). To each SNP we assigned its PIP computed using the locus in which it was most central. We have publicly released the PIPs and the prior and posterior means and variances of the causal effect sizes for all SNPs and traits analyzed.

PolyFun + SuSiE identified: 3,025 fine-mapped SNP–trait pairs with  $PIP > 0.95$ , a  $>32\%$  improvement versus SuSiE; 9,684 SNP–trait pairs with  $PIP > 0.5$ , an improvement of  $>59\%$  versus SuSiE; and 225,153 SNP–trait pairs with  $PIP > 0.05$ , an improvement of  $>84\%$  versus SuSiE (Supplementary Table 9). The number of SNPs with  $PIP > 0.95$  per trait ranged from 0 (number of children) to 407 (height) (Fig. 2a and Supplementary Table 9). The 3,025 SNP–trait pairs with  $PIP > 0.95$  spanned 2,225 unique SNPs, including 532 low-frequency SNPs ( $0.005 < MAF < 0.05$ ) and 185 rare SNPs ( $0.001 < MAF < 0.005$ ) (Supplementary Table 10). Only 39% of the

**Table 2 | Summary of mismatched reference LD simulations**

Expt	GWAS	LD	Generative SNPs	SNPs analyzed	Max. <i>L</i>
a	44K UK	44K UK (44,000 overlap)	UKB	UKB	10
b	44K UK	44K UK	UKB	UKB	10
c	44K UK	4K UK	UKB	UKB	10
d	44K UK	400 UK	UKB	UKB	1
e	44K UK	None	UKB	UKB	1
f	293K UK	44K UK	UKB	UKB	10
g	293K UK	4K UK	UKB	UKB	2
h	293K UK	4K UK (4,000 overlap)	UKB	UKB	2
i	44K EUR	44K UK	UKB	UKB	3
j	44K EUR	4K UK	UKB	UKB	2
k	44K EUR	400 UK	UKB	UKB	1
l	22K EUR + 22K UK	44K UK (22,000 overlap)	UKB	UKB	3
m	44K UK-REL	44K UK	UKB	UKB	10
n	44K EUR-REL	44K UK	UKB	UKB	3
o	44K UK	3.6K UK10K	UKB	UK10K $\cap$ UKB	-
p	44K UK	3.6K UK10K	UK10K $\cap$ UKB	UK10K $\cap$ UKB	2
q	44K UK	3.6K UK10K	UK10K $\cap$ UKB $\cap$ INF	UK10K $\cap$ UKB $\cap$ INF	10
r	44K UK	3.6K UK10K	UK10K $\cap$ UKB $\cap$ COM	UK10K $\cap$ UKB $\cap$ COM	1
s	44K UK	4K UK	UK10K $\cap$ UKB	UK10K $\cap$ UKB	10

For each experiment (Expt) we report: GWAS: the sample size and population of the target sample (UK denotes British-ancestry individuals from the UK Biobank; EUR denotes non-British European-ancestry individuals from UK Biobank; REL indicates that pairs of related individuals are included in the sample). LD: the sample size and population of the LD reference panel (UK denotes British-ancestry individuals from UK Biobank; UK10K denotes individuals from the UK10K cohort; numbers in parentheses indicate how many individuals overlap the target sample, if any. 'None' indicates that there is no LD reference panel). Generative SNPs: the set of SNPs from which we sampled causal SNPs (UKB: the set of UK Biobank-imputed SNPs with INFO score >0.6 and UKB MAF >0.1%. UK10K: the set of UK10K SNPs. INF: the set of UKB-imputed SNPs with INFO score >0.9. COM: the set of UKB-imputed SNPs with MAF >1% in British-ancestry individuals). SNPs analyzed: the set of SNPs that was used for fine-mapping. Max. *L*: the maximum number of causal SNPs per locus assumed by PolyFun + SuSiE that maintain FDR <0.05 at a threshold of PIP = 0.95 (selected from the options 1, 2, 3 and 10; - indicates that none of these options maintains FDR <0.05). Horizontal lines indicate the partitioning into types of experiments described in the Supplementary Note. Numerical results are reported in Supplementary Table 7.

2,225 SNPs with PIP > 0.95 were also lead GWAS SNPs (defined as SNPs with MAF > 0.001 and  $P < 5 \times 10^{-8}$  and no SNP with MAF > 0.001 and a smaller  $P$  value within 1 Mb) (Supplementary Table 10), demonstrating the importance of using fine-mapped SNPs rather than lead GWAS SNPs for downstream analysis. Of the SNPs with PIP > 0.95, 31% resided in coding regions and 22% were nonsynonymous (broadly consistent with previous fine-mapping studies<sup>8,12</sup>) (Supplementary Table 10). When restricting the analysis to 16 genetically uncorrelated traits ( $|r_g| < 0.2$ ; Methods and Supplementary Tables 11 and 12) we identified 1,626 SNP–trait pairs with PIP > 0.95 spanning 1,496 unique SNPs, with a median distance of 9 kb between an SNP with PIP > 0.95 and the nearest lead GWAS SNP for the same trait (Supplementary Table 10). The 16 genetically uncorrelated traits included 5,314 genome-wide-significant locus–trait pairs (defined by 1-Mb windows around lead GWAS SNPs) harboring 0.28 SNPs with PIP > 0.95 per locus on average (Supplementary Table 13); 1,080 of the 5,314 locus–trait pairs (20%) harbored  $\geq 1$  SNP(s) with PIP > 0.95, harboring 1.37 SNPs with PIP > 0.95 on average (Supplementary Table 13). Of the 1,626 SNP–trait pairs identified by PolyFun + SuSiE, 150 (9.2%) did not lie within genome-wide-significant loci, and 161 of the 1,626 SNP–trait pairs (9.9%) had  $P > 5 \times 10^{-8}$  (Supplementary Table 10).

We estimated the SNP heritability ( $h_g^2$ ) tagged by fine-mapped SNPs with PIP > 0.95 (which is probably close to the heritability causally explained by these SNPs, if most of the tagged SNP heritability originates from SNPs with PIP > 0.95). The  $h_g^2$  tagged by SNPs with PIP > 0.95 captured a large proportion of the  $h_g^2$  tagged by lead GWAS SNPs (median proportion = 42%; Fig. 2b; Methods and Supplementary Table 14). This proportion was substantially larger than the proportion of GWAS loci harboring SNPs with

PIP > 0.95 (20%; see above), because fine-mapping power is higher at loci with larger causal effects (Supplementary Table 4). However, fine-mapped SNPs tagged a smaller proportion of the total  $h_g^2$  causally explained by all genome-wide SNPs with MAF > 0.001 (median proportion = 19%; Fig. 2b; Methods and Supplementary Table 14), indicating that substantially larger sample sizes are required to comprehensively fine-map all heritable SNP effects.

Among the 2,225 unique SNPs with PIP > 0.95 fine-mapped for at least one trait, 223 were fine-mapped for multiple genetically uncorrelated traits (selecting a different subset of genetically uncorrelated traits for each SNP; Methods), including 55 SNPs fine-mapped for  $\geq 3$  genetically uncorrelated traits, indicating pervasive pleiotropy (Extended Data Fig. 6 and Supplementary Table 15); 118 pleiotropic SNPs resided in coding regions and 93 were nonsynonymous (Supplementary Table 15). The 17 SNPs fine-mapped for at least 4 traits are reported in Table 3. Previous studies have reported that genetically uncorrelated traits often share association signals at the same loci<sup>32</sup>, but did not fine-map those signals to individual SNPs as performed here.

To better understand the improvement of PolyFun + SuSiE over SuSiE, we examined the 121 loci where PolyFun + SuSiE identified a fine-mapped common SNP (PIP > 0.95) but SuSiE did not (PIP < 0.5 for all SNPs within 1 Mb) (Fig. 3 and Supplementary Table 16). In each case, functional annotations prioritized one SNP out of several candidates, greatly improving fine-mapping resolution.

We validated the motivation for performing functionally informed fine-mapping by verifying that fine-mapped SNPs are enriched for functional annotations, as previously shown for autoimmune diseases<sup>7,8,10</sup> and blood traits<sup>12</sup> (using nonfunctionally informed SuSiE to avoid biasing the results). For each of 50 main

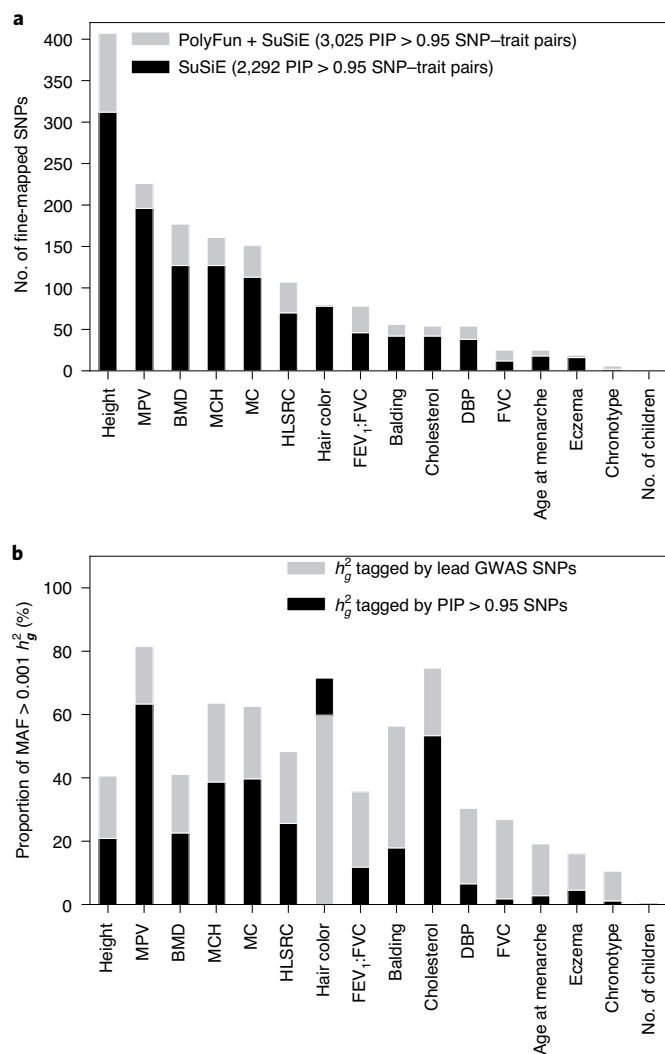


**Fig. 2 | Summary of fine-mapping results for UK Biobank traits. a**, The number of SNPs with PIP > 0.95 identified by SuSiE (black bars) and PolyFun + SuSiE (gray bars) across 16 genetically uncorrelated traits in the UK Biobank. Traits are ordered by PolyFun + SuSiE results. The numbers in the legend refer to the sum of all 49 traits analyzed. **b**, The proportion of SNP heritability causally explained by all genome-wide SNPs with MAF > 0.001 ( $h_g^2$ ) that is tagged by lead GWAS SNPs (gray bars) and by PolyFun + SuSiE SNPs with PIP > 0.95 (black bars). Traits are ordered as in **a**. For hair color, the  $h_g^2$  tagged by SNPs with PIP > 0.95 is  $>h_g^2$  tagged by lead GWAS SNPs. BMD, bone mineral density; DBP, diastolic blood pressure; FEV<sub>1</sub>:FVC, ratio of forced expiratory volume in 1 s to forced vital capacity; HLSRC, high light scatter reticulocyte count; MC, monocyte count, MCH: mean corpuscular hemoglobin; MPV, mean platelet volume. Numerical results are reported in Supplementary Tables 9 and 14.

binary annotations from the baseline-LF model<sup>24</sup>, for various PIP ranges, we computed the functional enrichment of fine-mapped common SNPs in the PIP range, defined as the proportion of common SNPs in the PIP range lying in the annotation divided by the proportion of genome-wide common SNPs lying in the annotation, and meta-analyzed the results across genetically uncorrelated traits (Methods; Fig. 4 and Supplementary Table 17). SNPs with PIP > 0.95 were strongly and significantly enriched for nonsynonymous SNPs (51× enrichment,  $P = 6.8 \times 10^{-185}$ ) and SNPs in conserved regions (16× enrichment,  $P < 10^{-300}$ ), significantly enriched for SNPs in various regulatory annotations (for example, promoter-ExAC

and H3K4me3), and significantly depleted for SNPs in repressed regions, consistent with previous literature on functional enrichment of fine-mapped SNPs<sup>7,8,10–12</sup> and disease heritability<sup>17,24,25,33</sup>. We observed qualitatively similar but weaker enrichments at lower PIP ranges (Fig. 4 and Supplementary Table 17).

We compared our fine-mapping results with those of two previous studies. First, we compared our results with ref. <sup>12</sup>, which performed nonfunctionally informed fine-mapping for 9 blood cell traits using approximately 115,000 of the individuals included in our analyses. PolyFun + SuSiE identified 4.4× more SNPs than ref. <sup>12</sup>, including all 4 SNPs that were functionally validated via luciferase reporter assays in ref. <sup>12</sup> (PIP > 0.999 for all 4 SNPs; Methods and Supplementary Tables 18–20). Second, we compared our results with those of ref. <sup>7</sup>, which performed nonfunctionally informed fine-mapping for seven of our traits, using a nonfunctionally informed method (PICS) and independent smaller datasets. PolyFun + SuSiE identified 35× more SNPs than ref. <sup>7</sup> (Supplementary Tables 21 and 22). Further details of the comparison are provided in the Supplementary Note.

We performed a further six secondary analyses, described in the Supplementary Note, Extended Data Figs. 7–9, and Supplementary Tables 10 and 23–28.

In summary, we leveraged the improved power of PolyFun + SuSiE to robustly identify thousands of fine-mapped SNPs, providing a rich set of potential candidates for functional follow-up. Our results further indicate pervasive pleiotropy, with many SNPs fine-mapped for two or more genetically uncorrelated traits.

**Polygenic localization of 49 complex traits.** SNPs with PIP > 0.95 tag a large proportion of the SNP heritability ( $h_g^2$ ) tagged by lead GWAS SNPs (median proportion = 42%) but a small proportion of total genome-wide  $h_g^2$  (median proportion = 19%) (Fig. 2b), implying that they causally explain a small proportion of  $h_g^2$ . We thus propose polygenic localization, which has the aim of identifying a minimal set of common SNPs causally explaining a specified proportion of common SNP heritability. A key difference between polygenic localization and previous studies of polygenicity<sup>34–38</sup> is that polygenic localization aims to identify (not just characterize) such SNPs.

Given a ranking of SNPs by posterior per-SNP heritability (that is, the posterior mean of their squared effect size; Methods), we define  $M_{50\%}$  as the size of the smallest set of top-ranked common SNPs causally explaining 50% of common SNP heritability (respectively  $M_p$  for proportion  $p$  of common SNP heritability). We estimate  $M_{50\%}$  (respectively  $M_p$ ) by: (1) partitioning SNPs into 50 ranked bins of similar posterior per-SNP heritability estimates from PolyFun + SuSiE and stratifying the lowest-heritability bin into 10 equally sized MAF bins, yielding 59 bins; (2) running S-LDSC using a different set of samples to re-estimate the average per-SNP heritability in each bin; and (3) computing the number of top-ranked common SNPs (with respect to the original ranking) whose estimated per-SNP heritabilities (from step 2) sum up to 50% (respectively the proportion  $p$ ) of the total estimated SNP heritability. We refer to this method as PolyLoc. The analysis of new samples in step 2 of PolyLoc prevents winner's curse; although PolyFun + SuSiE is robust to winner's curse, PolyLoc would be susceptible to it if it reused the data analyzed by PolyFun + SuSiE. We note that  $M_{50\%}$  relies on an empirical ranking and is thus larger than the size of the smallest set of SNPs causally explaining 50% of common SNP heritability, denoted as  $M_{50\%}^*$  ( $M_{50\%} \geq M_{50\%}^*$ ). We performed extensive simulations to confirm that PolyLoc produced robust upper bounds for  $M_{50\%}^*$  (Supplementary Note and Supplementary Tables 29 and 30). Further details of PolyLoc are provided in Methods; we have released open-source software implementing PolyLoc.

We applied PolyLoc to the 49 complex traits from the UK Biobank (Supplementary Table 8). We ranked SNPs using  $n = 337,000$  unrelated British-ancestry samples (steps 1 and 2)

**Table 3 | Pleiotropic fine-mapped SNPs for UK Biobank traits**

SNP	Position	MAF	Closest gene(s)	Annotation	Traits
rs13107325	chr4:103188709	0.08	<i>SLC39A8</i>	Nonsynonymous	BMI, balding, cholesterol, DBP, FVC, height, RBC, WHR (8)
rs1229984	chr4:100239319	0.02	<i>ADH1B</i>	Nonsynonymous	BMI, LDL, MCH, MPV, SBP, vitamin D (6)
rs76895963	chr12:4384844	0.02	<i>CCND2, CCND2-AS1</i>	Conserved	BMD, height, RBC, SBP, triglycerides (5)
rs140584594	chr1:110232983	0.27	<i>GSTM1</i>	Nonsynonymous	HDL, height, MC, MPV (4)
rs3811444	chr1:248039451	0.33	<i>TRIM58</i>	Nonsynonymous	HLSRC, HbA1c, platelet count, RBC (4)
rs1260326	chr2:27730940	0.39	<i>GCKR</i>	Nonsynonymous	Cholesterol, height, platelet count, RBCDW (4)
rs2270894	chr3:9975386	0.2	<i>CRELD1, IL17RC</i>	Conserved	BMD, FEV <sub>1</sub> /FVC, height, platelet count (4)
rs11556924	chr7:129663496	0.39	<i>ZC3HC1</i>	Nonsynonymous	Age at menarche, cardiovascular, height, platelet count (4)
rs3918226	chr7:150690176	0.08	<i>NOS3</i>	Conserved	Eczema, height, high cholesterol, MPV (4)
rs150813342	chr9:135864513	0.01	<i>GF1B</i>	Conserved	Eosinophil count, HLSRC, MCH, platelet count (4)
rs964184	chr11:116648917	0.13	<i>ZPR1</i>	DHS	Cholesterol, MPV, RBCDW, vitamin D (4)
rs35979828	chr12:54685880	0.07	<i>NFE2</i>	Conserved	Eosinophil count, platelet count, RBC, RBCDW (4)
rs2277339	chr12:57146069	0.1	<i>PRIM1</i>	Nonsynonymous	Height, LC, RBC, RBCDW (4)
rs72681869	chr14:50655357	0.01	<i>SOS2</i>	Nonsynonymous	FVC, hair color, HbA1c, SBP (4)
rs61745086	chr16:88782050	0.01	<i>PIEZO1, CTU2</i>	Nonsynonymous	HLSRC, HbA1c, height, RBC (4)
rs34557412	chr17:16852187	0.01	<i>TNFRSF13B</i>	Nonsynonymous	HbA1c, MC, MPV, RBC (4)
rs77542162	chr17:67081278	0.02	<i>ABCA6</i>	Nonsynonymous	HbA1c, height, LDL, platelet count (4)

We report SNPs fine-mapped (PIP > 0.95) for  $\geq 4$  genetically uncorrelated traits ( $|r_g| < 0.2$ ). For each SNP we report its name (SNP), position (hg19), MAF in the UK Biobank, closest gene(s) (using data from the GWAS catalog<sup>43</sup>), top annotation (Methods) and fine-mapped traits (and number of fine-mapped traits). SNPs are ordered first by the number of fine-mapped traits and then by genomic position. BMI, body mass index; cardiovascular: cardiovascular-related disease; cholesterol: total cholesterol; DBP, diastolic blood pressure; HbA1c, glycated hemoglobin; HDL, HDL-cholesterol; HLSRC, high light scatter reticulocyte count; LC, lymphocyte count; MC, monocyte count; MCH, mean corpuscular hemoglobin; MPV, mean platelet volume; RBC, red blood cell count; RBCDW, red blood cell distribution width; SBP, systolic blood pressure; WHR, waist:hip ratio (adjusted for BMI). Results for all 223 pleiotropic fine-mapped SNPs are reported in Supplementary Table 15.

and re-estimated average per-SNP heritabilities in each of 59 SNP bins using S-LDSC applied to  $n = 122,000$  European-ancestry UK Biobank samples that were not included in the  $n = 337,000$  set to avoid winner's curse (step 3). Estimates of  $M_{50\%}$  ranged widely from 28 (hair color) to 3,400 (height) to 2 million (number of children) (Fig. 5 and Supplementary Table 31). The median estimate of  $M_{50\%}$  across 16 genetically uncorrelated traits was 8,900; the median estimate of  $M_{5\%}$  was 8; and the median estimate of  $M_{95\%}$  was 4.4 million (of 7.0 million total common SNPs) (Supplementary Table 31). Pigmentation traits were the least polygenic traits whereas number of children was the most polygenic trait, having an  $M_{50\%}$  3.7 $\times$  larger than the second most polygenic of the 16 independent traits (chromotype, having an  $M_{50\%} = 553,000$ ), consistent with ref.<sup>34</sup> We performed seven secondary analyses, described in the Supplementary Note and Supplementary Tables 32 and 33. We note that far fewer than 2 million SNPs may causally explain 50% of the common SNP heritability of number of children, because  $M_{50\%}$  is a (possibly loose) upper bound.

Our results demonstrate that half of the common SNP heritability of complex traits is causally explained typically by thousands of SNPs (median  $M_{50\%} = 8,900$ ), and the remaining heritability is spread across an extremely large number of extremely weak-effect SNPs (median  $M_{95\%} = 4.4$  million), consistent with extremely polygenic but heavy-tailed trait architectures<sup>1,34–36,39–43</sup>.

## Discussion

We have introduced PolyFun, a framework that improves fine-mapping by prioritizing variants that are initially more likely to be causal based on their functional annotations. Across 49 UK Biobank traits, PolyFun + SuSiE confidently fine-mapped 3,025 SNP–trait pairs (PIP > 0.95), a 32% increase over nonfunctionally informed SuSiE. Of the fine-mapped SNPs, 223 were fine-mapped for multiple genetically uncorrelated traits, indicating pervasive pleiotropy. We further leveraged the results of PolyFun to perform polygenic localization by constructing minimal SNP sets causally

explaining a given proportion of common SNP heritability, demonstrating that 50% of common SNP heritability can be explained by sets ranging in size from 28 (hair color) to 3,400 (height) to 2 million (number of children). We note that these set sizes impose a (possibly loose) upper bound on the size of the smallest sets causally explaining 50% of common SNP heritability. We have publicly released the PIPs and the prior and posterior means and variances of effect sizes for all SNPs and traits analyzed.

We recommend applying PolyFun using in-sample LD from the GWAS target sample (that is, using exactly the same samples in both the target and reference samples), assuming ten causal SNPs per locus; we have facilitated this option for UK Biobank researchers by publicly releasing summary LD information for  $n = 337,000$  British-ancestry UK Biobank samples. As a second-best option we recommend applying PolyFun using an LD reference panel from the target sample population, spanning at least 10% of the target sample size, while assuming ten causal SNPs per locus. However, we caution that even subtle population differences may lead to false-positive results. Hence, our published summary LD information files are unsuitable for analysis of summary statistics involving non-British UK Biobank individuals, or data from other cohorts or consortia<sup>44–46</sup>. However, researchers may use larger subsets of UK Biobank data to identify genome-wide-significant loci, which they can fine-map using summary statistics and LD reference data based on  $n = 337,000$  British-ancestry individuals. In the absence of a reference panel from the target sample population spanning >10% of the target sample size, we recommend applying PolyFun without using an LD reference panel, by restricting it to assume a single causal SNP per locus.

Our fine-mapping analysis differs from several previous fine-mapping studies in two aspects. First, we applied PolyFun genome wide. However, we envision that the PolyFun software will primarily be used to fine-map genome-wide-significant loci, which harbor most SNPs with PIP > 0.95. We discuss possible reasons for identifying SNPs with PIP > 0.95 and  $P > 5 \times 10^{-8}$  in

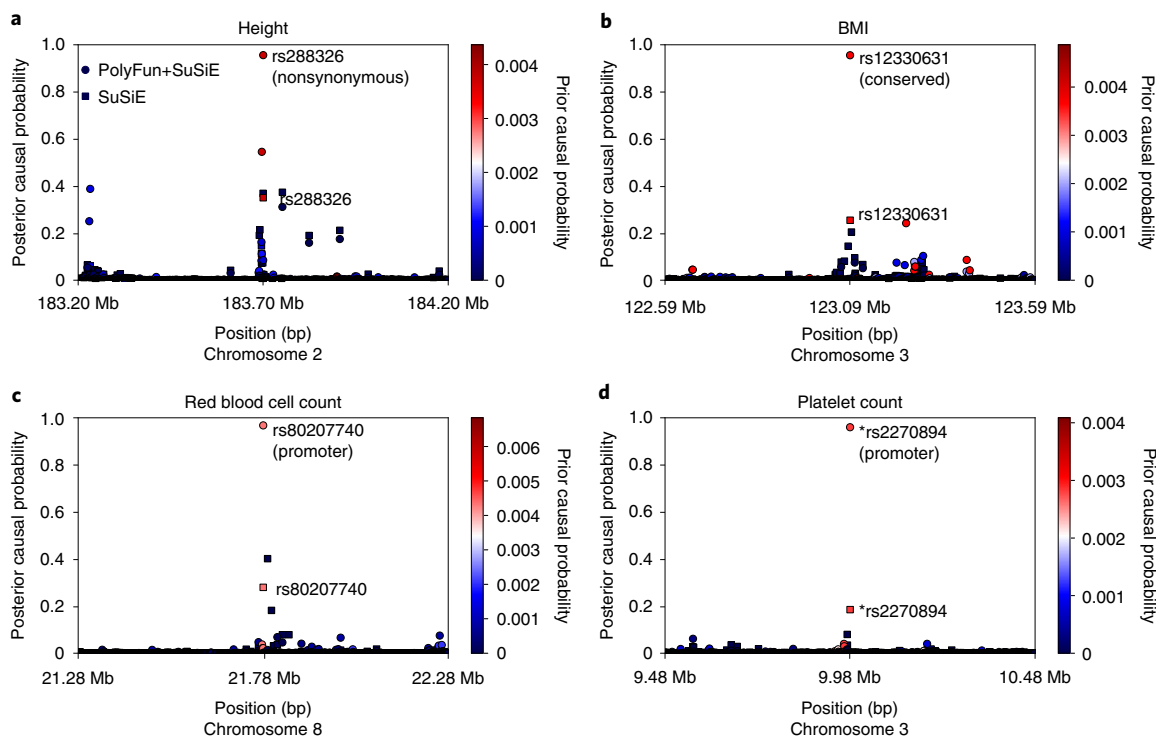


**Fig. 3 | Examples of the advantages of functionally informed fine-mapping for UK Biobank traits. a–d.** We report four examples where PolyFun + SuSiE identified a fine-mapped common SNP (PIP > 0.95) but SuSiE did not (PIP < 0.5 for all SNPs within 1 Mb) in four traits: height (a), BMI (b), red blood cell count (c) and platelet count (d). Circles denote PolyFun + SuSiE PIPs and squares denote SuSiE PIPs. SNPs are shaded according to their prior causal probabilities as estimated by PolyFun. The top PolyFun + SuSiE SNP is labeled (next to its PolyFun + SuSiE PIP and its SuSiE PIP). The annotation of each top PolyFun + SuSiE SNP that is most enriched among SuSiE SNPs with PIP > 0.95 (Methods) is reported in parentheses below its label. Asterisks denote lead GWAS SNPs. Numerical results are reported in Supplementary Table 16.

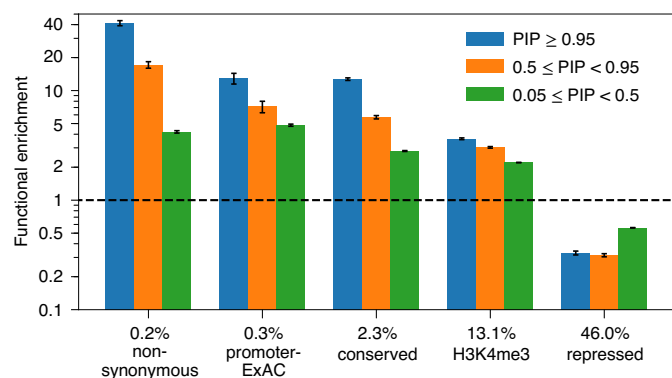


**Fig. 4 | Functional enrichment of SuSiE fine-mapped common SNPs for UK Biobank traits.** We report the functional enrichment of fine-mapped common SNPs (defined as the proportion of common SNPs with a PIP range lying in an annotation divided by the proportion of genome-wide common SNPs lying in the annotation) for 5 selected binary annotations, meta-analyzed across 14 genetically uncorrelated UK Biobank traits with  $\geq 10$  SNPs with PIP > 0.95 (log scale). The proportion of common SNPs lying in each binary annotation is reported above its name. The horizontal dashed line denotes no enrichment. Error bars denote the s.e. Numerical results for all 50 main binary annotations and all traits are reported in Supplementary Table 17.

the Supplementary Note. Second, PolyFun fine-maps all signals in a locus jointly to maximize power<sup>5,28</sup>. Researchers wishing to use PolyFun for a partitioned analysis<sup>47</sup> may still do so by first partitioning a locus into multiple signals using a separate tool

(for example, GCTA-COJO<sup>47</sup>) and then applying PolyFun to each signal separately, restricting PolyFun to assume a single causal SNP per signal.

Our results provide several opportunities for future work. First, the fine-mapped SNPs that we identified could be prioritized for functional follow-up. Second, fine-mapping results (posterior mean effect sizes) can be used to compute transethnic polygenic risk scores<sup>48</sup> which may be less sensitive to LD differences between populations than existing methods<sup>49,50</sup>. Third, the proximal pairs of coding and noncoding fine-mapped SNPs that we identified (Supplementary Table 25) may aid efforts to link SNPs to genes<sup>51–53</sup>. Fourth, SNPs that were fine-mapped for multiple genetically uncorrelated traits may shed light on shared biological pathways<sup>54</sup>. Fifth, sets of SNPs causally explaining 50% of common SNP heritability can potentially be used for gene and pathway enrichment analysis<sup>55,56</sup>. Finally, PolyFun can incorporate additional functional annotations at negligible additional computational cost, motivating further efforts to identify conditionally informative annotations.

Our work has several limitations. First, our estimates of the FDR of PIP > 0.95 SNPs in PolyFun and other methods are conservative, demonstrating the challenges of exact calibration in fine-mapping. Second, subtle population stratification may lead to spurious fine-mapping results<sup>57</sup>. However, our fine-mapped SNPs are concentrated in associated loci with larger estimated effects, which are relatively less likely to be spurious. Third, we restricted fine-mapping to  $n = 337,000$  unrelated British-ancestry individuals, consistent with previous studies<sup>12</sup>. Hence, our published summary LD information files do not support fine-mapping of UK Biobank data that include non-British individuals. Fourth, PolyLoc requires analyzing samples distinct from the samples analyzed by PolyFun to avoid winner’s curse. Researchers with access to individual-level genetic

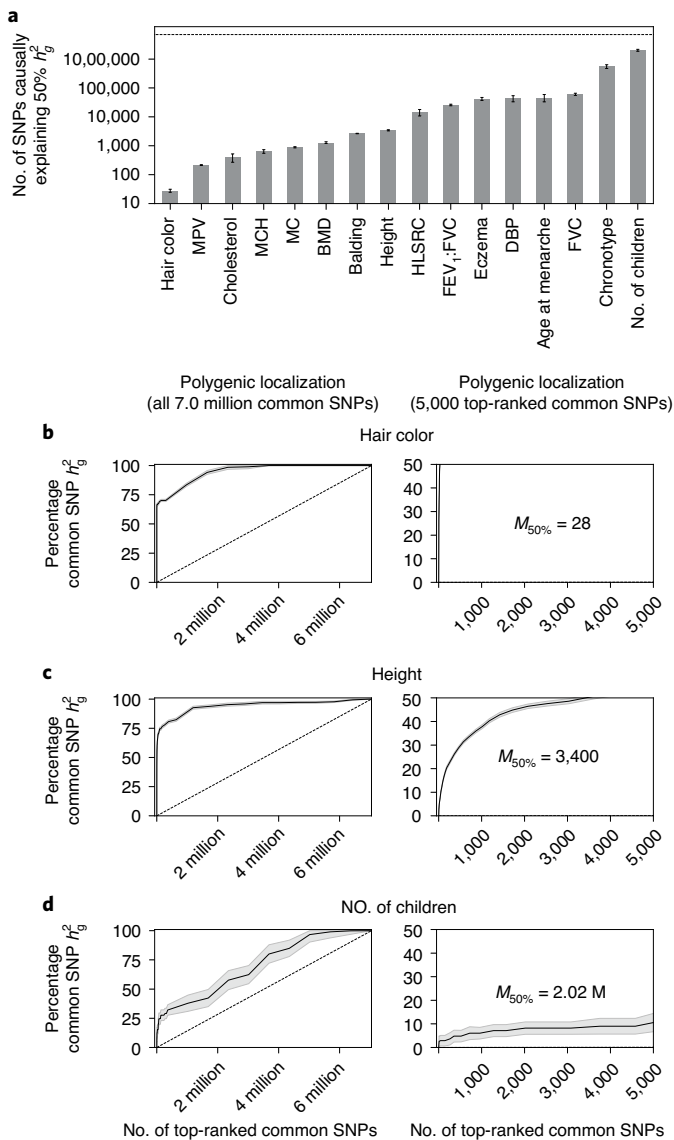


**Fig. 5 | Polygenic localization results for UK Biobank traits.** **a**,  $M_{50\%}$  estimates across 16 genetically uncorrelated traits. For each trait, we report the number of top-ranked common SNPs (using PolyFun + SuSiE posterior per-SNP heritability estimates for ranking) causally explaining 50% of common SNP heritability, and its s.e. (log scale). The horizontal dashed line denotes the total number of common SNPs in the analysis (7.0 million). **b–d**, The proportion of common SNP heritability of hair color (**b**), height (**c**) and number of children (**d**) explained by different numbers of top-ranked SNPs, for all 7.0 million common SNPs (left) and the 5,000 top-ranked common SNPs (right). Gray shading denotes the s.e. Dashed black lines denote a null model with a constant per-SNP heritability. We also report the number of top-ranked SNPs causally explaining 50% of common SNP heritability, denoted as  $M_{50\%}$ . Discontinuities in the slope indicate transitions between SNP bins. Numerical results for all 49 UK Biobank traits are reported in Supplementary Table 31.

data can partition the samples as we have done (we recommend using approximately 75% of the data for fine-mapping and 25% for polygenic localization). Fifth, PolyFun does not support X-chromosome analysis. Sixth, PolyLoc provides only an upper bound on the proportion of SNPs causally explaining a given proportion of SNP heritability. Finally, multiethnic fine-mapping<sup>58</sup> and incorporation of tissue-specific functional annotations<sup>9,13,15,17</sup> may

further increase fine-mapping power. Incorporating these into our fine-mapping framework is an avenue for future work.

### Online content

Any methods, additional references, Nature Research reporting summaries, source data, extended data, supplementary information, acknowledgements, peer review information; details of author contributions and competing interests; and statements of data and code availability are available at <https://doi.org/10.1038/s41588-020-00735-5>.

Received: 28 October 2019; Accepted: 2 October 2020;  
Published online: 16 November 2020

### References

1. Visscher, P. M. et al. 10 years of GWAS discovery: biology, function, and translation. *Am. J. Hum. Genet.* **101**, 5–22 (2017).
2. Shendure, J., Findlay, G. M. & Snyder, M. W. Genomic medicine—progress, pitfalls, and promise. *Cell* **177**, 45–57 (2019).
3. Schaid, D. J., Chen, W. & Larson, N. B. From genome-wide associations to candidate causal variants by statistical fine-mapping. *Nat. Rev. Genet.* **19**, 491–504 (2018).
4. The Wellcome Trust Case Control Consortium et al. Bayesian refinement of association signals for 14 loci in 3 common diseases. *Nat. Genet.* **44**, 1294–1301 (2012).
5. Hormozdiari, F., Kostem, E., Kang, E. Y., Pasianic, B. & Eskin, E. Identifying causal variants at loci with multiple signals of association. *Genetics* **198**, 497–508 (2014).
6. Chen, W. et al. Fine mapping causal variants with an approximate Bayesian method using marginal test statistics. *Genetics* **200**, 719–736 (2015).
7. Farh, K. K.-H. et al. Genetic and epigenetic fine mapping of causal autoimmune disease variants. *Nature* **518**, 337–343 (2015).
8. Huang, H. et al. Fine-mapping inflammatory bowel disease loci to single-variant resolution. *Nature* **547**, 173–178 (2017).
9. Mahajan, A. et al. Refining the accuracy of validated target identification through coding variant fine-mapping in type 2 diabetes. *Nat. Genet.* **50**, 559–571 (2018).
10. Mahajan, A. et al. Fine-mapping type 2 diabetes loci to single-variant resolution using high-density imputation and islet-specific epigenome maps. *Nat. Genet.* **50**, 1505–1513 (2018).
11. Westra, H.-J. et al. Fine-mapping and functional studies highlight potential causal variants for rheumatoid arthritis and type 1 diabetes. *Nat. Genet.* **50**, 1366–1374 (2018).
12. Ulirsch, J. C. et al. Interrogation of human hematopoiesis at single-cell and single-variant resolution. *Nat. Genet.* **51**, 683–693 (2019).
13. Maurano, M. T. et al. Systematic localization of common disease-associated variation in regulatory DNA. *Science* **337**, 1190–1195 (2012).
14. The ENCODE Project Consortium. An integrated encyclopedia of DNA elements in the human genome. *Nature* **489**, 57–74 (2012).
15. Trynka, G. et al. Chromatin marks identify critical cell types for fine mapping complex trait variants. *Nat. Genet.* **45**, 124–130 (2013).
16. The Roadmap Epigenomics Consortium. Integrative analysis of 111 reference human epigenomes. *Nature* **518**, 317–330 (2015).
17. Finucane, H. K. et al. Partitioning heritability by functional annotation using genome-wide association summary statistics. *Nat. Genet.* **47**, 1228–1235 (2015).
18. Kichaev, G. et al. Integrating functional data to prioritize causal variants in statistical fine-mapping studies. *PLoS Genet.* **10**, e1004722 (2014).
19. Kichaev, G. et al. Improved methods for multi-trait fine mapping of pleiotropic risk loci. *Bioinformatics* **33**, 248–255 (2017).
20. Chen, W., McDonnell, S. K., Thibodeau, S. N., Tillmans, L. S. & Schaid, D. J. Incorporating functional annotations for fine-mapping causal variants in a Bayesian framework using summary statistics. *Genetics* **204**, 933–958 (2016).
21. Wang, G., Sarkar, A., Carbonetto, P. & Stephens, M. A simple new approach to variable selection in regression, with application to genetic fine mapping. *J. R. Stat. Soc. Series B* <https://doi.org/10.1111/rssb.12388> (2020).
22. Benner, C. et al. FINEMAP: efficient variable selection using summary data from genome-wide association studies. *Bioinformatics* **32**, 1493–1501 (2016).
23. Benner, C., Havulinna, A., Salomaa, V., Ripatti, S. & Pirinen, M. Refining fine-mapping: effect sizes and regional heritability. Preprint at *bioRxiv* <https://doi.org/10.1101/318618> (2018).
24. Gazal, S. et al. Linkage disequilibrium-dependent architecture of human complex traits shows action of negative selection. *Nat. Genet.* **49**, 1421–1427 (2017).
25. Gazal, S. et al. Functional architecture of low-frequency variants highlights strength of negative selection across coding and non-coding annotations. *Nat. Genet.* **50**, 1600–1607 (2018).

26. Gazal, S., Marquez-Luna, C., Finucane, H. K. & Price, A. L. Reconciling S-LDSC and LDK functional enrichment estimates. *Nat. Genet.* **51**, 1202–1204 (2019).
27. Bycroft, C. et al. The UK Biobank resource with deep phenotyping and genomic data. *Nature* **562**, 203–209 (2018).
28. Benner, C. et al. Prospects of fine-mapping trait-associated genomic regions by using summary statistics from genome-wide association studies. *Am. J. Hum. Genet.* **101**, 539–551 (2017).
29. Pasaniuc, B. & Price, A. L. Dissecting the genetics of complex traits using summary association statistics. *Nat. Rev. Genet.* **18**, 117–127 (2017).
30. Marquez-Luna, C. et al. Modeling functional enrichment improves polygenic prediction accuracy in UK Biobank and 23andMe data sets. Preprint at *bioRxiv* <https://doi.org/10.1101/375337> (2019).
31. Loh, P.-R., Kichaev, G., Gazal, S., Schoech, A. P. & Price, A. L. Mixed-model association for biobank-scale datasets. *Nat. Genet.* **50**, 906–908 (2018).
32. Pickrell, J. K. et al. Detection and interpretation of shared genetic influences on 42 human traits. *Nat. Genet.* **48**, 709–717 (2016).
33. Hujoel, M. L., Gazal, S., Hormozdiari, F., van de Geijn, B. & Price, A. L. Disease heritability enrichment of regulatory elements is concentrated in elements with ancient sequence age and conserved function across species. *Am. J. Hum. Genet.* **104**, 611–624 (2019).
34. O'Connor, L. J. et al. Extreme polygenicity of complex traits is explained by negative selection. *Am. J. Hum. Genet.* **105**, 456–476 (2019).
35. Zeng, J. et al. Signatures of negative selection in the genetic architecture of human complex traits. *Nat. Genet.* **50**, 746–753 (2018).
36. Zhang, Y., Qi, G., Park, J.-H. & Chatterjee, N. Estimation of complex effect-size distributions using summary-level statistics from genome-wide association studies across 32 complex traits. *Nat. Genet.* **50**, 1318–1326 (2018).
37. Zhu, X. & Stephens, M. Large-scale genome-wide enrichment analyses identify new trait-associated genes and pathways across 31 human phenotypes. *Nat. Commun.* **9**, 4361 (2018).
38. Moser, G. et al. Simultaneous discovery, estimation and prediction analysis of complex traits using a Bayesian mixture model. *PLoS Genet.* **11**, e1004969 (2015).
39. Yang, J. et al. Genetic variance estimation with imputed variants finds negligible missing heritability for human height and body mass index. *Nat. Genet.* **47**, 1114–20 (2015).
40. Purcell, S. M. et al. Common polygenic variation contributes to risk of schizophrenia and bipolar disorder. *Nature* **460**, 748–752 (2009).
41. Yang, J. et al. Common SNPs explain a large proportion of the heritability for human height. *Nat. Genet.* **42**, 565–569 (2010).
42. Loh, P.-R. et al. Contrasting genetic architectures of schizophrenia and other complex diseases using fast variance-components analysis. *Nat. Genet.* **47**, 1385–1392 (2015).
43. Boyle, E. A., Li, Y. I. & Pritchard, J. K. An expanded view of complex traits: from polygenic to omnigenic. *Cell* **169**, 1177–1186 (2017).
44. Wuttke, M. et al. A catalog of genetic loci associated with kidney function from analyses of a million individuals. *Nat. Genet.* **51**, 957–972 (2019).
45. Landi, M. T. et al. Genome-wide association meta-analyses combining multiple risk phenotypes provide insights into the genetic architecture of cutaneous melanoma susceptibility. *Nat. Genet.* **52**, 494–504 (2020).
46. Vujkovic, M. et al. Discovery of 318 new risk loci for type 2 diabetes and related vascular outcomes among 1.4 million participants in a multi-ancestry meta-analysis. *Nat. Genet.* **52**, 680–691 (2020).
47. Yang, J. et al. Conditional and joint multiple-SNP analysis of GWAS summary statistics identifies additional variants influencing complex traits. *Nat. Genet.* **44**, 369–375 (2012).
48. Chatterjee, N., Shi, J. & García-Closas, M. Developing and evaluating polygenic risk prediction models for stratified disease prevention. *Nat. Rev. Genet.* **17**, 392–406 (2016).
49. Márquez-Luna, C., Loh, P.-R. & Consortium, S. A. T. Multiethnic polygenic risk scores improve risk prediction in diverse populations. *Genet. Epidemiol.* **41**, 811–823 (2017).
50. Martin, A. R. et al. Clinical use of current polygenic risk scores may exacerbate health disparities. *Nat. Genet.* **51**, 584 (2019).
51. Claussnitzer, M. et al. FTO obesity variant circuitry and adipocyte browning in humans. *N. Engl. J. Med.* **373**, 895–907 (2015).
52. Jung, I. et al. A compendium of promoter-centered long-range chromatin interactions in the human genome. *Nat. Genet.* **51**, 1442–1449 (2019).
53. Zeggini, E., Gloyn, A. L., Barton, A. C. & Wain, L. V. Translational genomics and precision medicine: moving from the lab to the clinic. *Science* **365**, 1409–1413 (2019).
54. Solovieff, N., Cotsapas, C., Lee, P. H., Purcell, S. M. & Smoller, J. W. Pleiotropy in complex traits: challenges and strategies. *Nat. Rev. Genet.* **14**, 483–495 (2013).
55. Wang, K., Li, M. & Hakonarson, H. Analysing biological pathways in genome-wide association studies. *Nat. Rev. Genet.* **11**, 843–854 (2010).
56. De Leeuw, C. A., Neale, B. M., Heskes, T. & Posthuma, D. The statistical properties of gene-set analysis. *Nat. Rev. Genet.* **17**, 353–364 (2016).
57. Haworth, S. et al. Apparent latent structure within the UK Biobank sample has implications for epidemiological analysis. *Nat. Commun.* **10**, 333 (2019).
58. Kichaev, G. & Pasaniuc, B. Leveraging functional-annotation data in trans-ethnic fine-mapping studies. *Am. J. Hum. Genet.* **97**, 260–271 (2015).

**Publisher's note** Springer Nature remains neutral with regard to jurisdictional claims in published maps and institutional affiliations.

© The Author(s), under exclusive licence to Springer Nature America, Inc. 2020

## Methods

**PolyFun fine-mapping method.** PolyFun first estimates prior causal probabilities for all SNPs and then applies fine-mapping methods such as SuSiE<sup>21</sup> and FINEMAP<sup>22,23</sup> with these prior causal probabilities. Below, we describe estimation of the prior causal probabilities.

We model standardized phenotypes  $y$  using the linear model  $y = \sum_i x_i \beta_i + \epsilon$ , where  $x_i$  denotes standardized SNP genotypes,  $\beta_i$  denotes effect size and  $\epsilon$  is a residual term. We use a point-normal model for  $\beta_i$ :

$$\beta_i | \mathbf{a}_i \approx \begin{cases} \mathcal{N}(0, \text{var}[\beta_i | \beta_i \neq 0]) & \text{with probability } P(\beta_i \neq 0 | \mathbf{a}_i) \\ 0 & \text{otherwise,} \end{cases}$$

where  $\mathbf{a}_i$  are the functional annotations of SNP  $i$ ,  $P(\beta_i \neq 0 | \mathbf{a}_i)$  is its prior causal probability and  $\text{var}[\beta_i | \beta_i \neq 0]$  is its causal variance, which we assume is independent of  $\mathbf{a}_i$ . This assumption is motivated by our recent work showing that functional enrichment is primarily due to differences in polygenicity rather than differences in effect-size magnitude, which is constrained by negative selection<sup>34</sup>.

The key quantity that PolyFun uses to estimate prior causal probabilities is the per-SNP heritability of SNP  $i$ ,  $\text{var}[\beta_i | \mathbf{a}_i]$  (we refer to this quantity as per-SNP heritability because the total SNP heritability  $\text{var}[\sum_i x_i \beta_i | \mathbf{a}]$  is equal to  $\sum_i \text{var}[\beta_i | \mathbf{a}_i]$ , assuming that causal SNP effects have zero mean and are uncorrelated with other SNP effects and with other SNPs conditional on  $\mathbf{a}$ ). PolyFun relates the prior causal probability  $P(\beta_i \neq 0 | \mathbf{a}_i)$  to the per-SNP heritability  $\text{var}[\beta_i | \mathbf{a}_i]$  via the law of total variance:

$$P(\beta_i \neq 0 | \mathbf{a}_i) = \frac{\text{var}[\beta_i | \mathbf{a}_i]}{\text{var}[\beta_i | \beta_i \neq 0]}. \quad (2)$$

Equation (1) in the main text follows because  $P(\beta_i \neq 0 | \mathbf{a}_i)$  is proportional to  $\text{var}[\beta_i | \mathbf{a}_i]$  with the proportionality factor  $1/\text{var}[\beta_i | \beta_i \neq 0]$ .

To derive equation (2) we define the causality indicator  $c_i = \mathbb{1}[\beta_i \neq 0 | \mathbf{a}_i]$  and apply the law of total variance to  $\text{var}[\beta_i | \mathbf{a}_i]$ :

$$\begin{aligned} \text{var}[\beta_i | \mathbf{a}_i] &= E_{c_i}[\text{var}[\beta_i | \mathbf{a}_i, c_i]] + \text{var}_{c_i}[E[\beta_i | \mathbf{a}_i, c_i]] \\ &= E_{c_i}[\text{var}[\beta_i | \mathbf{a}_i, c_i]] + \text{var}_{c_i}[0] \\ &= P(c_i = 0) \times 0 + P(c_i = 1) \text{var}[\beta_i | \mathbf{a}_i, c_i = 1] \\ &= P(\beta_i \neq 0 | \mathbf{a}_i) \text{var}[\beta_i | \mathbf{a}_i, \beta_i \neq 0] \\ &= P(\beta_i \neq 0 | \mathbf{a}_i) \text{var}[\beta_i | \beta_i \neq 0]. \end{aligned}$$

The last equality holds because we assume that the causal effect size variance is independent of functional annotations, as explained above.

PolyFun avoids directly estimating the proportionality factor  $1/\text{var}[\beta_i | \beta_i \neq 0]$  by constraining the prior causal probabilities  $P(\beta_i \neq 0 | \mathbf{a}_i)$  in each tested locus to sum to 1.0. This constraint implies that each locus is initially expected to harbor one causal SNP, consistent with previous fine-mapping methods<sup>6,22</sup> (this constraint is ignored by PolyFun + SuSiE because it is invariant to scaling of prior causal probabilities). Hence, the main challenge is estimating the per-SNP heritabilities  $\text{var}[\beta_i | \mathbf{a}_i]$ .

To estimate  $\text{var}[\beta_i | \mathbf{a}_i]$ , PolyFun incorporates a regularized extension of S-LDSC with the baseline-LF model<sup>17,24–26</sup>, which we extend to a new version 2.2.UKB (Supplementary Table 1 and see below). S-LDSC uses the linear model  $\text{var}[\beta_i | \mathbf{a}_i] = \sum_c \tau^c a_i^c$  and jointly estimates all  $\tau^c$  parameters by minimizing the term  $\sum_i (\chi_i^2 - n \sum_c \tau^c l(i, c) - nb - 1)^2$ , where  $c$  iterates over functional annotations,  $\tau^c$  is the coefficient of annotation  $c$ ,  $\chi_i^2$  is the  $\chi^2$  statistic of SNP  $i$ ,  $n$  is the sample size,  $b$  measures the contribution of confounding biases and  $l(i, c) = \sum_j r_{ij}^2 a_j^c$ .

Although S-LDSC produces robust estimates of functional enrichment, it has two limitations in estimating  $\text{var}[\beta_i | \mathbf{a}_i]$ : (1) these estimates can have a large s.e. in the presence of many annotations, and (2) the model may not be robust to model misspecification. To address the first limitation, PolyFun incorporates an L2-regularized extension of S-LDSC. To address the second limitation, PolyFun employs special procedures to ensure robustness to model misspecification. The key idea is to approximate arbitrary complex functional forms of  $\text{var}[\beta_i | \mathbf{a}_i]$  via a piecewise-constant function. To do this, PolyFun partitions SNPs with similar estimated values of  $\text{var}[\beta_i | \mathbf{a}_i]$  (estimated via a possibly misspecified model) into nonoverlapping bins, estimates the SNP heritability causally explained by each bin  $b$ , and specifies  $\text{var}[\beta_i | \mathbf{a}_i]$  for SNPs in bin  $b$  as the SNP heritability causally explained by bin  $b$  divided by the number of SNPs in bin  $b$ . PolyFun avoids winner's curse by using different data for partitioning SNPs and for per bin heritability estimation.

In detail, PolyFun robustly specifies prior causal probabilities for all SNPs on a target locus on a corresponding odd (respectively even) target chromosome via the following procedure:

- Estimate annotation coefficients  $\hat{\tau}_{\text{even}}^c$  and intercepts  $\hat{b}_{\text{even}}$  using only SNPs in even chromosomes via an L2-regularized extension of S-LDSC that minimizes  $\sum_i (\chi_i^2 - n \sum_c \hat{\tau}_{\text{even}}^c l(i, c) - n \hat{b}_{\text{even}} - 1)^2 + \lambda \sum_c (\hat{\tau}_{\text{even}}^c)^2$  (respectively using  $\hat{\tau}_{\text{odd}}^c$  and  $\hat{b}_{\text{odd}}$ ). We select the regularization strength  $\lambda$  from a geometrically spaced grid of 100 values ranging from  $10^{-8}$  to 100, selecting the one that minimizes the average out-of-chromosome error  $\sum_r \sum_{i \in r} (\chi_i^2 - n \sum_c \hat{\tau}_{\text{even}/r}^c l(i, c) - n \hat{b}_{\text{even}/r} - 1)^2$ , where  $r$  iterates over even (respectively odd) chromosomes, and  $\hat{\tau}_{\text{even}/r}^c$ ,  $\hat{b}_{\text{even}/r}$  are the S-LDSC  $\tau$  and

$b$  estimates, respectively, when applied to all SNPs on even chromosomes except for chromosome  $r$  (respectively for odd chromosomes).

- Compute per-SNP heritabilities  $\widehat{\text{var}}[\beta_i | \mathbf{a}_i] = \sum_c \hat{\tau}_{\text{even}}^c a_i^c$  for each SNP  $i$  in an odd chromosome (respectively  $\sum_c \hat{\tau}_{\text{odd}}^c a_i^c$ ).
- Partition all SNPs into 20 bins with similar values of  $\widehat{\text{var}}[\beta_i | \mathbf{a}_i]$  using the Ckmedian.1d.dp method<sup>39</sup>. This method partitions SNPs into 20 maximally homogeneous bins such that the average distance of  $\widehat{\text{var}}[\beta_i | \mathbf{a}_i]$  to the median  $\widehat{\text{var}}[\beta_i | \mathbf{a}_i]$  of the bin of SNP  $i$  is minimized. Even though this step uses functional annotations data of the target chromosome, it does not use the summary statistics of SNPs in the target chromosome, which ensures robustness to winner's curse.
- Apply S-LDSC with non-negativity constraints to estimate per-SNP heritabilities in each of the 20 bins of all SNPs in odd (respectively even) chromosomes except for the target chromosome  $r$  (to avoid using the same data that will be used in fine-mapping), denoted  $\hat{\sigma}_{r,1}^2, \dots, \hat{\sigma}_{r,20}^2$ . Afterwards, regularize the estimates by setting all values smaller than  $q \times \max_b (\hat{\sigma}_{r,b}^2)$  to  $q \times \max_b (\hat{\sigma}_{r,b}^2)$ , using  $q = 1/100$  by default, and rescaling the  $\hat{\sigma}_{r,b}^2$  estimates to have the same sum (over all genome-wide SNPs) as before. The regularization prevents SNPs from having a zero per-SNP heritability, which would exclude them from fine-mapping. We did not apply L2 regularization in this step because we require approximately unbiased estimates, and because the s.e. values are relatively small under a small number of nonoverlapping annotations.
- Specify a prior causal probability proportional to  $\hat{\sigma}_{r,b}^2$  for each SNP that is in bin  $b$  and resides in a target locus in chromosome  $r$ , such that the prior causal probabilities in the target locus sum to one.

PolyFun uses v.2.2.UKB of the baseline-LF model, which differs from the original baseline-LF model<sup>25</sup> by including SNPs with MAF  $\geq 0.001$  and several new annotations, and omitting annotations that could not be easily extended to account for SNPs with MAF  $< 0.005$  (Supplementary Table 1). Briefly, we use 187 overlapping functional annotations, including 10 common MAF bins (MAF  $\geq 0.05$ ), 10 low-frequency MAF bins ( $0.05 > \text{MAF} \geq 0.001$ ), 6 LD-related annotations for common SNPs (levels of LD, predicted allele age, recombination rate, nucleotide diversity, background selection statistic, CpG content), 5 LD-related annotations for low-frequency SNPs, 40 binary functional annotations for common SNPs, 7 continuous functional annotations for common SNPs, 40 binary functional annotations for low-frequency SNPs, 3 continuous functional annotations for low-frequency SNPs and 66 annotations constructed via windows around other annotations<sup>17</sup>. We did not include a base annotation that includes all SNPs, because such an annotation is linearly dependent on all the MAF bins when S-LDSC uses the same set of SNPs to compute LD scores and to estimate annotation coefficients.

**Main fine-mapping simulations.** We simulated summary statistics for 18,212,157 genotyped and imputed autosomal SNPs with MAF  $\geq 0.001$  and INFO score  $\geq 0.6$  (including short indels, excluding three long-range LD regions; see below), using  $n = 337,491$  unrelated British-ancestry individuals from UK Biobank release 3. In most simulations we computed an effect variance  $\beta_i$  for every SNP  $i$  with annotations  $\mathbf{a}_i$ , using the baseline-LF (v.2.2.UKB) model,  $\text{var}[\beta_i | \mathbf{a}_i] = \sum_c \tau^c a_i^c$ , where  $c$  is an annotation and  $\tau^c$  estimates are taken from a fixed-effects meta-analysis of 16 well-powered, genetically uncorrelated ( $|r_g| < 0.2$ ) UK Biobank traits, scaled such that  $\sum_i \text{var}[\beta_i | \mathbf{a}_i]$  is the same across all traits (Supplementary Table 3). In some simulations we generated values of  $\text{var}[\beta_i | \mathbf{a}_i]$  under alternative functional architectures to evaluate the robustness of PolyFun to modeling misspecification (Supplementary Note). Each SNP was set to be causal with probability proportional to  $\text{var}[\beta_i | \mathbf{a}_i]$ , such that the average causal probability was equal to the desired proportion of causal SNPs. We provide technical details about the simulations in the Supplementary Note.

We performed fine-mapping in each of the ten selected 3-Mb loci on chromosome 1 using methods based on SuSiE<sup>21</sup>, FINEMAP<sup>22,23</sup>, CAVIARBF<sup>20</sup> and fastPAINTOR<sup>19</sup>. Following previous literature<sup>12,28</sup> all methods used in-sample LD (that is, summary LD information based on the genotypes of the same 337,491 individuals used to generate summary statistics), computed via LDstore<sup>28</sup>. For fastPAINTOR-, fastPAINTOR, SuSiE and PolyFun + SuSiE, we specified a causal effect size variance using an estimator that we developed based on a modified version of HESS<sup>60</sup> rather than using the estimator implemented in these methods, because it improved FDR and power in most simulation settings (Supplementary Note and Supplementary Table 4).

We ran SuSiE v.0.7.1.0487 with default values for all parameters except the following: (1) we used ten causal SNPs per locus; and (2) we estimated a per-locus causal effect size variance (the scaled\_prior\_variance parameter) via our modified HESS approach. We specified prior causal probabilities via the prior\_weights parameter. We modified the SuSiE source code to avoid performing the LD matrix diagnostics (positive definiteness and symmetry) because they greatly increased memory consumption.

We ran FINEMAP v.1.3.1.b with a maximum of ten causal SNPs per locus and with default settings for all other parameters. We specified prior causal probabilities via the --prior-snps argument.

We ran CAVIARBF v.0.2.1 with an Akaike information criterion-based parameter selection, using ridge regression with regularization parameter  $\lambda$

selected from  $\{2^{-10}, 2^{-5}, 2^{-2.5}, 2^0, 2^{2.5}, 2^5, 100, 1000, 10000, 100000\}$ , with a single locus and up to either one or two causal SNPs per locus, owing to computational limitations.

We ran fastPAINTOR v.3.1 in MCMC mode. We specified a per-locus causal effect size variance (specified via the  $-variance$  argument) using our modified HESS approach (as in PolyFun + SuSiE). We avoided truncating the LD matrix (using `prop_ld_eigenvalues = 1.0`) because we used in-sample summary LD information. As fastPAINTOR is generally not designed to work with more than 10 annotations<sup>18,19</sup> (and was too slow in our simulations to estimate the significance of each annotation and include only conditionally significant annotations as done in ref. <sup>18</sup>), we selected a subset of ten highly informative annotations by: (1) scoring each annotation based on its average contribution to effect variance  $|a_i^2 \tau^2|$  across all SNPs, using the true  $\tau$  of the generative model; and (2) iteratively selecting top-ranked annotations such that no annotation has correlation  $>0.3$  (in absolute value) with a previously selected annotation, until selecting ten annotations. We determined that ten annotations yielded approximately optimal power while maintaining correct calibration (Supplementary Table 4).

For each PIP threshold, we conservatively estimated FDRs by setting all PIPs greater than the threshold to the threshold, yielding a uniform false-discovery threshold (Supplementary Note and Supplementary Table 4).

We computed  $P$  values of FDR differences and power differences of analyses with perturbed PolyFun steps via a Wald test, using a jackknife over simulated datasets to estimate the s.e. (Supplementary Note).

**Simulations with mismatched reference LD.** Our mismatched reference LD simulations differed from our main simulations in several ways: (1) we generated summary statistics using up to  $n = 44,000$  unrelated (or related) European-ancestry (British or non-British) UK Biobank target samples in most experiments, compared with  $n = 320,000$  in our main simulations, because the UK Biobank includes only 44,000 unrelated UK Biobank individuals of non-British European ancestry (we used  $n = 293,000$  unrelated British-ancestry UK Biobank target samples in a subset of experiments to more closely match our main simulations); (2) we computed summary LD information using  $n = 400$ ,  $n = 4,000$  or  $n = 44,000$  unrelated British-ancestry UK Biobank reference samples (either nonoverlapping or overlapping with the target samples), or using  $n = 3,567$  reference samples from the UK10K cohort<sup>61</sup> (compared with in-sample LD based on the target samples in the main simulations); (3) we generated summary statistics using individual-level genotypes rather than summary LD information (as required when the target sample and the LD reference panel are not the same); (4) we simulated three causal SNPs per locus that jointly explain 0.5% of trait variance, compared with ten causal SNPs that jointly explain 0.05% of trait variance in our main simulations, to obtain sufficient power despite having a smaller sample size; and (5) in some experiments we used a subset of SNPs for generating causal SNPs or for fine-mapping analysis. We provide technical details of these simulations in the Supplementary Note.

### Functionally informed fine-mapping of 49 complex traits in the UK Biobank.

We applied SuSiE and PolyFun + SuSiE to fine-map 49 traits in the UK Biobank, using the same data and the same parameter settings described in Main fine-mapping simulations. We performed basic quality control on each trait as described in our previous publications<sup>30,31</sup>. Specifically, we removed outliers outside the reasonable range for each quantitative trait, and applied quantile normalizing within-sex strata after correcting for covariates for nonbinary traits with non-normal distributions. We computed summary statistics with BOLT-LMM v.2.3.3 (ref. <sup>31</sup>) adjusting for sex, age and age squared, assessment center, genotyping platform and the top 20 principal components (computed as described in ref. <sup>31</sup>), and dilution factor for biochemical traits. As the noninfinitesimal version of BOLT-LMM does not estimate effect sizes, we computed  $z$ -scores for fine-mapping by taking the square root of the BOLT-LMM  $\chi^2$  statistics and multiplying them by the sign of the effect estimate from the infinitesimal version of BOLT-LMM.

We partitioned all autosomal chromosomes into 2,763 overlapping 3-Mb-long loci with 1 Mb spacing between the start points of consecutive loci. We computed a PIP for each SNP based on the locus with the center closest to the SNP (excluding SNPs  $>1$  Mb away from the closest center and loci wherein all SNPs had squared marginal effect sizes  $<0.00005$ ). We excluded the MHC region (chr6 25.5–33.5 M) and two other long-range LD regions (chr8 8–12 M, chr11 46–57 M)<sup>62</sup> from all analyses, following our observations that both FINEMAP and SuSiE tend to produce spurious results in these regions, finding many SNPs with PIP = 1 across many traits regardless of their BOLT-LMM  $P$  values. We verified that other previously reported long-range LD regions<sup>62</sup> do not harbor a disproportionate number of SNPs with PIP  $>0.95$ . We specified per-locus causal effect variances for SuSiE and PolyFun + SuSiE via our modified HESS approach. For all S-LDSC and fine-mapping analyses, we specified a sample size corresponding to the BOLT-LMM effective sample size<sup>31</sup> (given by the true sample size multiplied by the median ratio between  $\chi^2$  statistics of BOLT-LMM and linear regression across SNPs with BOLT-LMM  $\chi^2 > 30$ ).

All S-LDSC analyses used LD scores computed from in-sample summary LD information (based on imputed SNP dosages rather than sequenced genotypes as in previous publications<sup>24–26</sup>, assigning to each SNP the LD score computed in the locus in which it was most central), because they provide better coverage

of low-frequency SNPs and are consistent with the fine-mapping analyses. We computed genetic correlations with LDSC, using the same summary statistics used for fine-mapping and restricting the analysis to common SNPs.

We selected a subset of 16 genetically uncorrelated traits by ranking all traits according to the number of PolyFun + SuSiE SNPs with PIP  $>0.95$  and greedily selecting top-ranked traits such that no selected trait has  $|r_{g_i}| > 0.2$  with a previously selected trait, excluding traits having either (1)  $h_g^2$  estimates  $<0.05$  in either the PolyFun dataset ( $n = 337,000$ ) or the PolyLoc dataset ( $n = 122,000$ ) (see the  $h_g^2$  estimation description below) or (2) traits with an effective sample size  $<100,000$  in the  $n = 337,000$  dataset (using  $4/((1/\text{no. of cases}) + (1/\text{no. of controls}))$  for binary traits).

We estimated  $h_g^2$  tagged by SNPs with PIP  $>0.95$  and by lead GWAS SNPs via a multivariate linear regression. We regressed all the covariates used in BOLT-LMM out of the phenotypes, performed multivariate linear regression on the residuals (using all SNPs with PIP  $>0.95$  as explanatory variables) and reported the adjusted  $R^2$  as the  $h_g^2$  tagged by these SNPs. We verified that the results remained nearly identical regardless of whether we excluded related individuals (Supplementary Table 14). We estimated the heritability causally explained by all genome-wide SNPs with MAF  $>0.001$  for trait selection and for Fig. 2b by running S-LDSC with all the baseline-LF annotations. We overrode the automatic removal of very large-effect SNPs employed by S-LDSC for hair color, because this removal led to  $h_g^2$  estimates that were smaller than the linear regression-based estimates, due to the large proportion of SNP heritability originating from very large-effect SNPs.

We defined top annotations for Table 3, Fig. 3 and Supplementary Tables 15 and 16 by first ranking all annotations according to their functional enrichment among SNPs with PIP  $>0.95$  (as in Fig. 4; see below), and associating each SNP with its top-ranked annotation, using meta-analyzed enrichment.

We selected a subset of genetically uncorrelated traits for each SNP (used in Extended Data Fig. 6, Table 3 and Supplementary Table 15), aiming to select traits from as diverse a set of groups as possible (anthropometric, lipids/metabolic, blood, cardiovascular/metabolic disease, other; Extended Data Fig. 6 and Supplementary Table 8). To this end, we iterated over trait groups cyclically. For each group containing one or more unselected traits with PIP  $>0.95$  for the analyzed SNP, we selected the trait having the smallest average  $|r_{g_i}|$  with unselected traits from other groups (if there remained any) or from all remaining traits (otherwise), selecting among all traits having  $|r_{g_i}| < 0.2$  with previously selected traits, until no more eligible traits remained. We plotted the ideogram in Extended Data Fig. 6 using the PhenoGram<sup>33</sup> software.

We computed enrichment of functional annotations among fine-mapped SNPs (Fig. 4) as the ratio between the proportion of common SNPs with PIP above a given threshold having a specific annotation and the proportion of common SNPs having the annotation. We excluded continuous annotations and annotations constructed via windows around other annotations, and merged concordant annotations for common and low-frequency variants. We computed  $P$  values using Fisher's exact test (meta-analyzed across traits via Fisher's method). We computed the s.e. by: (1) computing the s.e.  $s$  of the log of the enrichment via the standard formula for the s.e. of relative risk (exploiting the fact that enrichment and relative risk are both ratios of proportions) and (2) computing the s.e. of the enrichment via  $\sqrt{r^2(e^{s^2} - 1)}$  (that is, the s.d. of the exponent of a normal random variable), where  $r$  is the original enrichment estimate (meta-analyzed across traits using a fixed-effect meta-analysis). We excluded traits having fewer than ten SNPs with PIP  $>0.95$  from the meta-analysis. The annotations shown in Fig. 4 are nonsynonymous, Conserved\_LindbladToh (denoted Conserved), Human\_Promoter\_Villar\_ExAC (denoted Promoter-ExAC), H3K4me3\_Trynka (denoted H3K4me3) and Repressed\_Hoffman (denoted Repressed) (see Supplementary Table 1 for details).

To compare our fine-mapping results with those of refs. <sup>7,12</sup>, we restricted the comparison to SNPs that were not excluded from our fine-mapping procedure (SNPs with MAF  $\geq 0.001$  in the UK Biobank  $n = 337,000$  dataset, INFO score  $\geq 0.6$ , distance  $<1$  Mb away from the closest locus center and not residing in one of the excluded long-range LD regions). When the same SNP had multiple reported PIPs in ref. <sup>12</sup>, we used the entry with the larger PIP. We caution that the comparison with ref. <sup>12</sup> is not a replication analysis because the datasets of ref. <sup>12</sup> and of PolyFun + SuSiE are correlated.

We selected five traits for down-sampling analysis (analyzing  $n = 107,000$  individuals) as the set of traits having: (1) the largest number of 3-Mb loci harboring a genome-wide-significant SNPs; (2)  $>10$  SNPs with PIP  $>0.95$  in the SuSiE  $n = 107,000$  analysis; and (3)  $|r_{g_i}| < 0.2$  with another selected trait.

**Polygenic localization.** Polygenic localization aims to identify a minimal set of SNPs causally explaining a given proportion of common SNP heritability. To define polygenic localization, we first define  $M_p$  as the smallest integer  $k$  such that  $\sum_{i \in \{s_1, \dots, s_k\}} \beta_i^2 / \sum_{i=1}^m \beta_i^2 \geq P$ , where  $\beta_i$  is a standardized SNP effect size,  $s_j$  denotes a ranking of  $\beta_i^2$  such that  $\beta_{s_1}^2 \geq \beta_{s_2}^2 \geq \dots \geq \beta_{s_m}^2$  and  $m$  is the number of common SNPs. Unfortunately,  $\beta_i^2$  is unknown in practice. Polygenic localization therefore estimates an upper bound of  $M_p$ , denoted as  $M_p$ . We define  $M_p$  as the smallest integer  $k'$  such that  $\sum_{i \in \{s'_1, \dots, s'_k\}} \beta_i^2 / \sum_{i=1}^m \beta_i^2 \geq P$ , where  $s'$  is a possibly nonoptimal ranking of SNPs. We note that  $M_p \geq M_p$  by construction. We provide a full derivation of polygenic localization in the Supplementary Note.

We now provide a brief conceptual description of PolyLoc (a full description is provided in the Supplementary Note). Briefly, PolyLoc proceeds by: (1) partitioning SNPs with similar  $\beta_i^2$  posterior mean estimates (using PolyFun + SuSiE estimates) into bins; (2) treating  $\beta_i$  as a zero-mean random variable and jointly estimating  $\text{var}[\beta_i]$  in every bin using S-LDSC; and (3) finding the smallest integer  $k$  such that  $\sum_{i \in \{\hat{s}_1, \dots, \hat{s}_k\}} \text{var}[\beta_i] / \sum_{i=1}^m \text{var}[\beta_i] \geq P$ , where  $\hat{s}_i$  denotes the original ranking of  $\beta_i^2$  posterior mean estimates from PolyFun + SuSiE. The use of  $\text{var}[\beta_i] = E[\beta_i^2] - E[\beta_i]^2$  instead of  $\beta_i^2$  uses the assumption that  $\beta_i$  has zero mean in each bin. The partitioning into bins in step 1 induces a piecewise-linear approximation of the function  $(k) = \sum_{i \in \{\hat{s}_1, \dots, \hat{s}_k\}} \beta_i^2 / \sum_{i=1}^m \beta_i^2$ . We use different datasets to estimate  $\beta_i^2$  posterior means and  $\text{var}[\beta_i]$  to prevent winner's curse. Our approach is conservative by design due to using an imperfect ranking compared with the true ranking  $s_1, \dots, s_m$ . The degree of conservativeness is a function of fine-mapping power, and thus depends on factors affecting fine-mapping power such as sample size, levels of LD at causal SNPs, MAFs of causal SNPs and trait polygenicity.

In secondary analyses, we compared PolyLoc with an alternative method that performs polygenic localization based on prior estimates of per-SNP heritability from functional annotations, rather than posterior estimates. This alternative method uses per-SNP heritability estimates and SNP bins from step 4 of PolyFun, based only on the  $n = 337,000$  dataset (noting that it does not suffer from winner's curse because PolyFun applies partitioning into odd and even chromosomes).

**Reporting summary.** Further information on research design is available in the Nature Research Reporting Summary linked to this article.

### Data availability

PolyFun fine-mapping results generated in the present study are available for public download at [http://data.broadinstitute.org/alkesgroup/polyfun\\_results](http://data.broadinstitute.org/alkesgroup/polyfun_results). Summary LD information generated in the present study is available for public download at [https://data.broadinstitute.org/alkesgroup/UKBB\\_LD\\_Baseline-LF\\_v2.2.UKB\\_annotations\\_and\\_LD\\_scores\\_for\\_UK\\_Biobank\\_SNPs](https://data.broadinstitute.org/alkesgroup/UKBB_LD_Baseline-LF_v2.2.UKB_annotations_and_LD_scores_for_UK_Biobank_SNPs). Access to the UK Biobank resource is available via application (<http://www.ukbiobank.ac.uk>).

### Code availability

PolyFun and PolyLoc software is available at <https://github.com/omerwe/polyfun>. SuSiE software is available at <https://github.com/stephenslab/susieR>. FINEMAP software is available at <http://www.christianbenner.com/#>.

### References

- Wang, H. & Song, M. Ckmeans.1d.dp: optimal k-means clustering in one dimension by dynamic programming. *R J.* **3**, 29–33 (2011).
- Shi, H., Kichaev, G. & Pasaniuc, B. Contrasting the genetic architecture of 30 complex traits from summary association data. *Am. J. Hum. Genet.* **99**, 139–53 (2016).
- The UK10K Consortium et al. The UK10K project identifies rare variants in health and disease. *Nature* **526**, 82–90 (2015).
- Price, A. L. et al. Long-range LD can confound genome scans in admixed populations. *Am. J. Hum. Genet.* **83**, 132–135 (2008).
- Wolfe, D., Dudek, S., Ritchie, M. D. & Pendergrass, S. A. Visualizing genomic information across chromosomes with PhenoGram. *BioData Min.* **6**, 18 (2013).
- Welter, D. et al. The NHGRI GWAS catalog, a curated resource of SNP-trait associations. *Nucleic Acids Res.* **42**, D1001–D1006 (2014).

### Acknowledgements

We thank B. Pasaniuc, G. Kichaev, M. Stephens, G. Wang, M. Kanai, B. M. Schilder and T. Raj for helpful discussions. This research was conducted using the UK Biobank Resource under application no. 16549 and was funded by National Institutes of Health grants (nos. U01 HG009379, R37 MH107649, R01 MH101244 and R01 HG006399) and the Academy of Finland grants (nos. 288509 and 312076). H.K.F. is supported by E. and W. Schmidt. Computational analyses were performed on the O2 High-Performance Compute Cluster at Harvard Medical School.

### Author contributions

O.W. and A.L.P. designed the study. O.W. and S.G. analyzed the data. C.B. extended the FINEMAP software. O.W. and A.L.P. wrote the manuscript with assistance from F.H., C.B., R.C., J.U., S.G., A.P.S., B.v.d.G., Y.R., C.M.L., L.O., M.P. and H.K.F.

### Competing interests

The authors declare no competing interests.

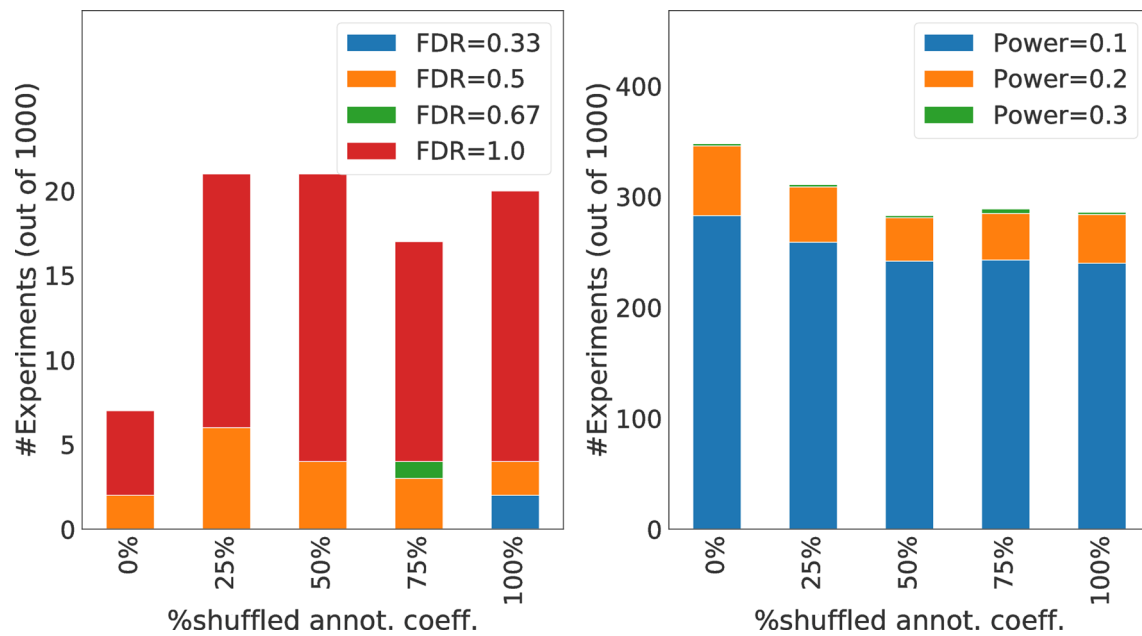
### Additional information

**Extended data** is available for this paper at <https://doi.org/10.1038/s41588-020-00735-5>.

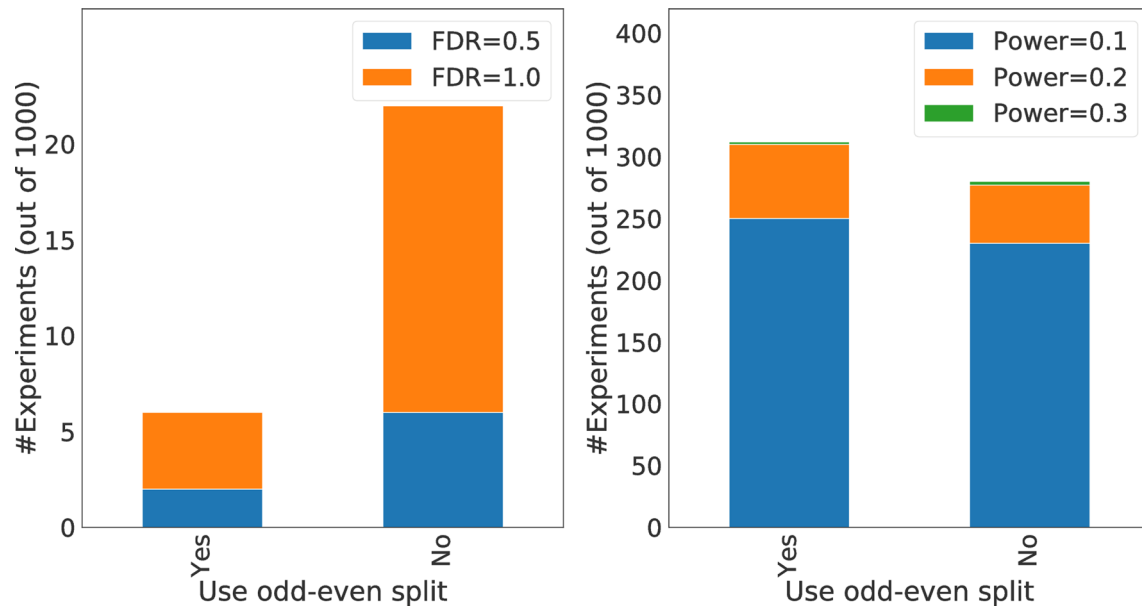
**Supplementary information** is available for this paper at <https://doi.org/10.1038/s41588-020-00735-5>.

**Correspondence and requests for materials** should be addressed to O.W. or A.L.P.

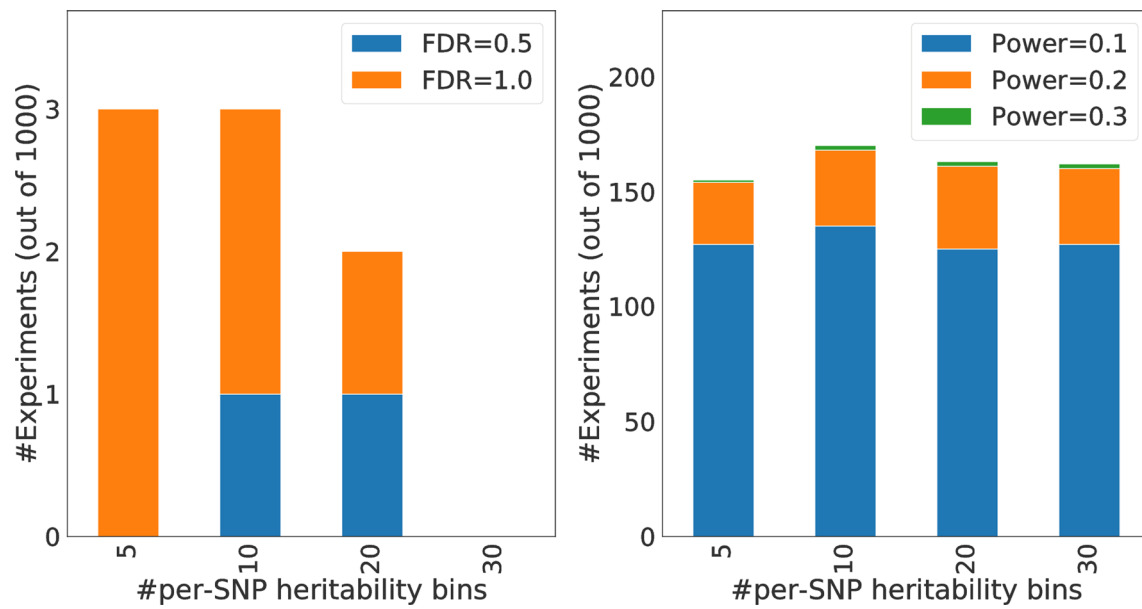
**Reprints and permissions information** is available at [www.nature.com/reprints](http://www.nature.com/reprints).



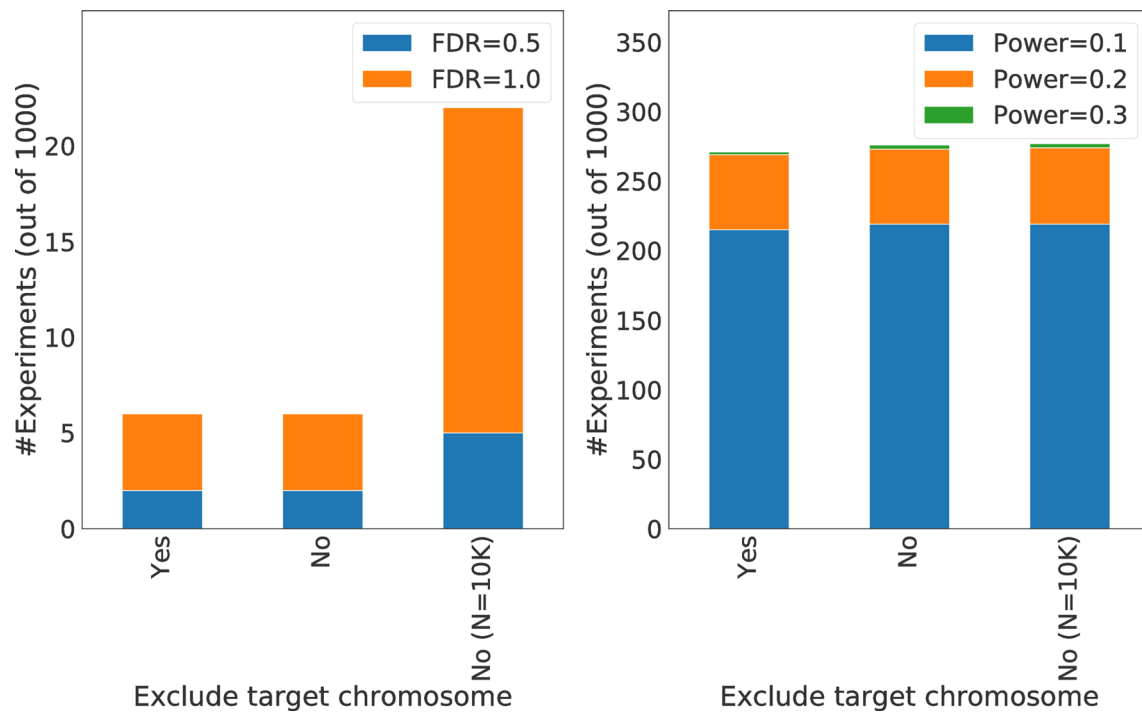
**Extended Data Fig. 1 | Assessing the individual impact of step 1 of PolyFun (estimating functional enrichment) via perturbation analysis, by randomly shuffling different proportions of annotation coefficient estimates.** For each evaluated value of the proportion of shuffled annotation coefficient estimates, we report the number of experiments having each obtained FDR level  $>0$  (left panel) and the number of experiments having each obtained power level  $>0$  (right panel), out of 1000 experiments. FDR and power are reported with respect to identifying  $PIP \geq 0.95$  SNPs. Experiments with FDR=0 (resp. power=0) are not reported in the left panel (resp. right panel) to improve clarity. Numerical reports are provided in Supplementary Table 6.



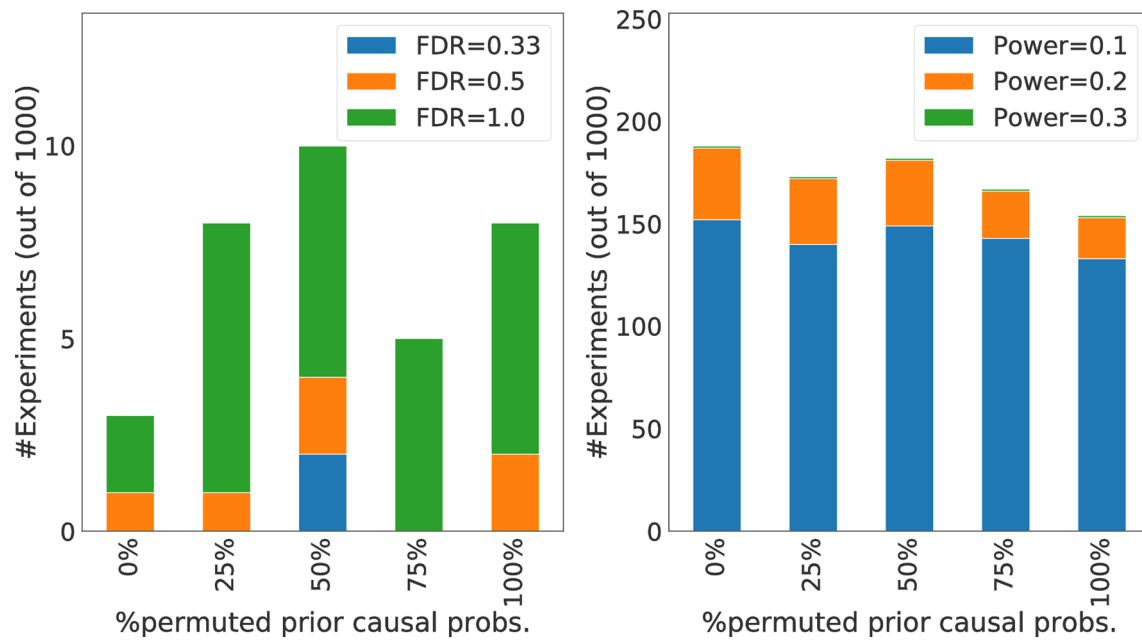
**Extended Data Fig. 2 | Assessing the individual impact of step 2 of PolyFun (estimating per-SNP heritabilities on odd/even chromosomes) via perturbation analysis, by using both odd and even chromosomes to estimate functional enrichment.** The figure is similar to Extended Data Figure 1 but applies a different perturbation (using both odd and even chromosomes to estimate functional enrichment). Numerical reports are provided in Supplementary Table 6.



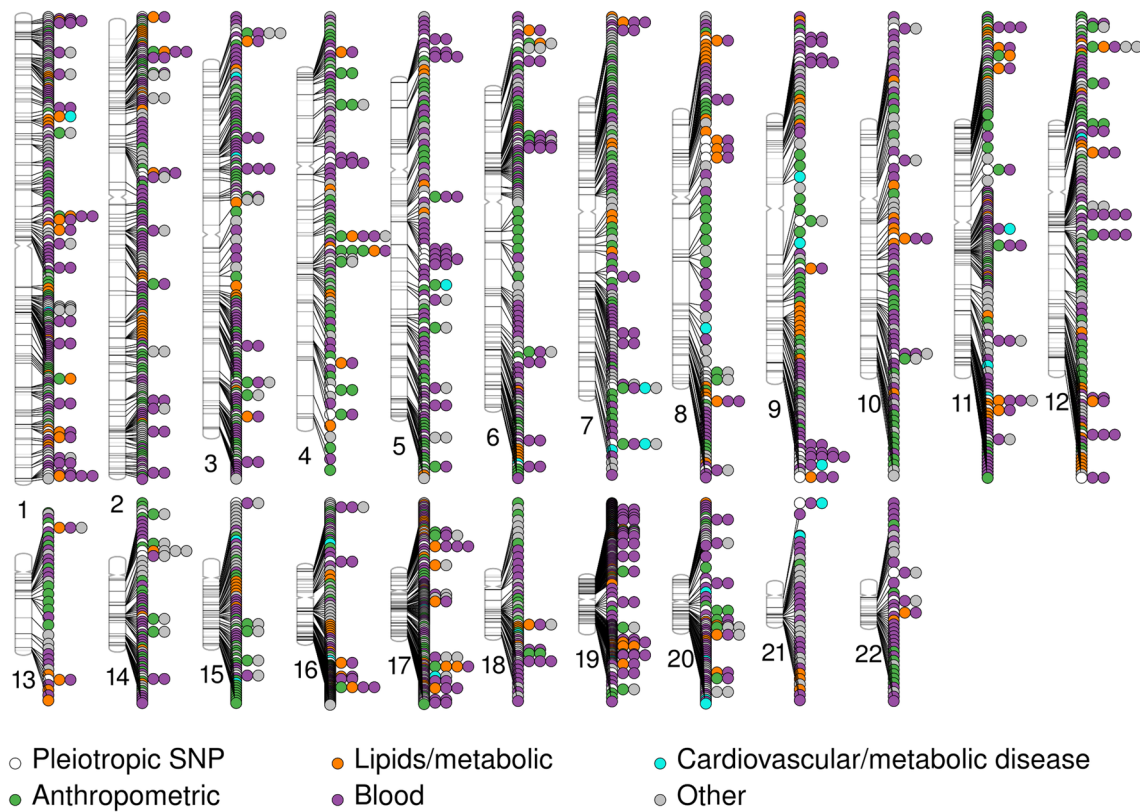
**Extended Data Fig. 3 | Assessing the individual impact of step 3 of PolyFun (partitioning all SNPs into 20 bins of similar per-SNP heritability) via perturbation analysis, by varying the number of per-SNP heritability bins.** The figure is similar to Extended Data Figure 1 but applies a different perturbation (changing the number of per-SNP heritability bins). Numerical reports are provided in Supplementary Table 6.



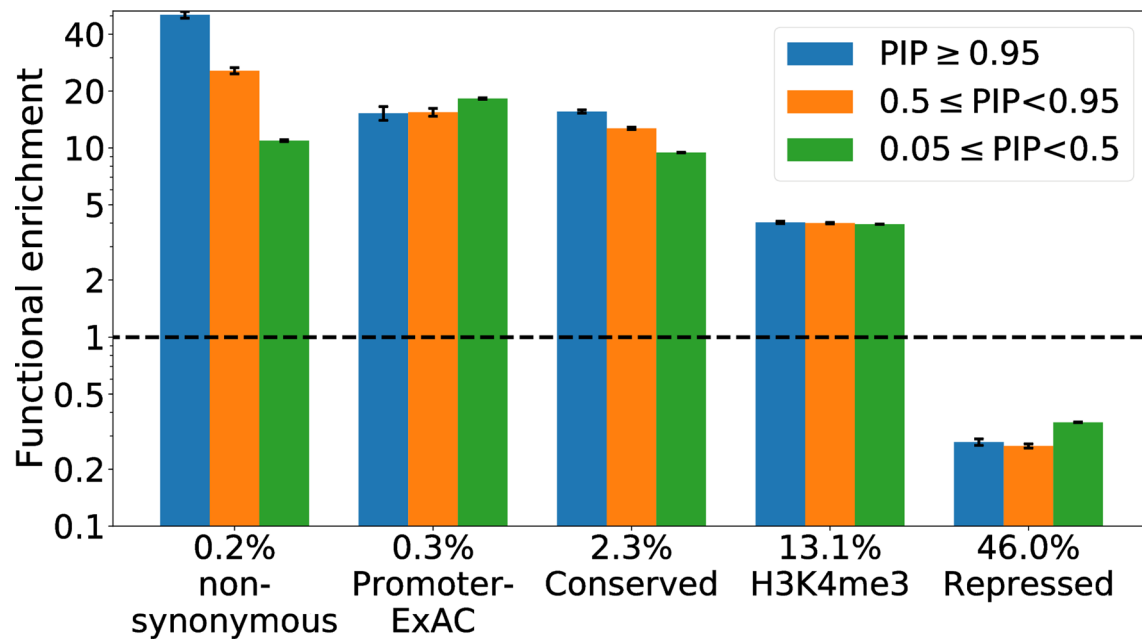
**Extended Data Fig. 4 | Assessing the individual impact of step 4 of PolyFun (re-estimating per-SNP heritabilities within each bin excluding the target chromosome) via perturbation analysis, by not excluding the target chromosome from the re-estimation procedure.** The figure is similar to Extended Data Figure 1 but applies a different perturbation (disables the exclusion of the target chromosome, either when using the default sample size  $N=320\text{ K}$  or when using a smaller sample size of  $N=10\text{ K}$ ). Numerical reports are provided in Supplementary Table 6.



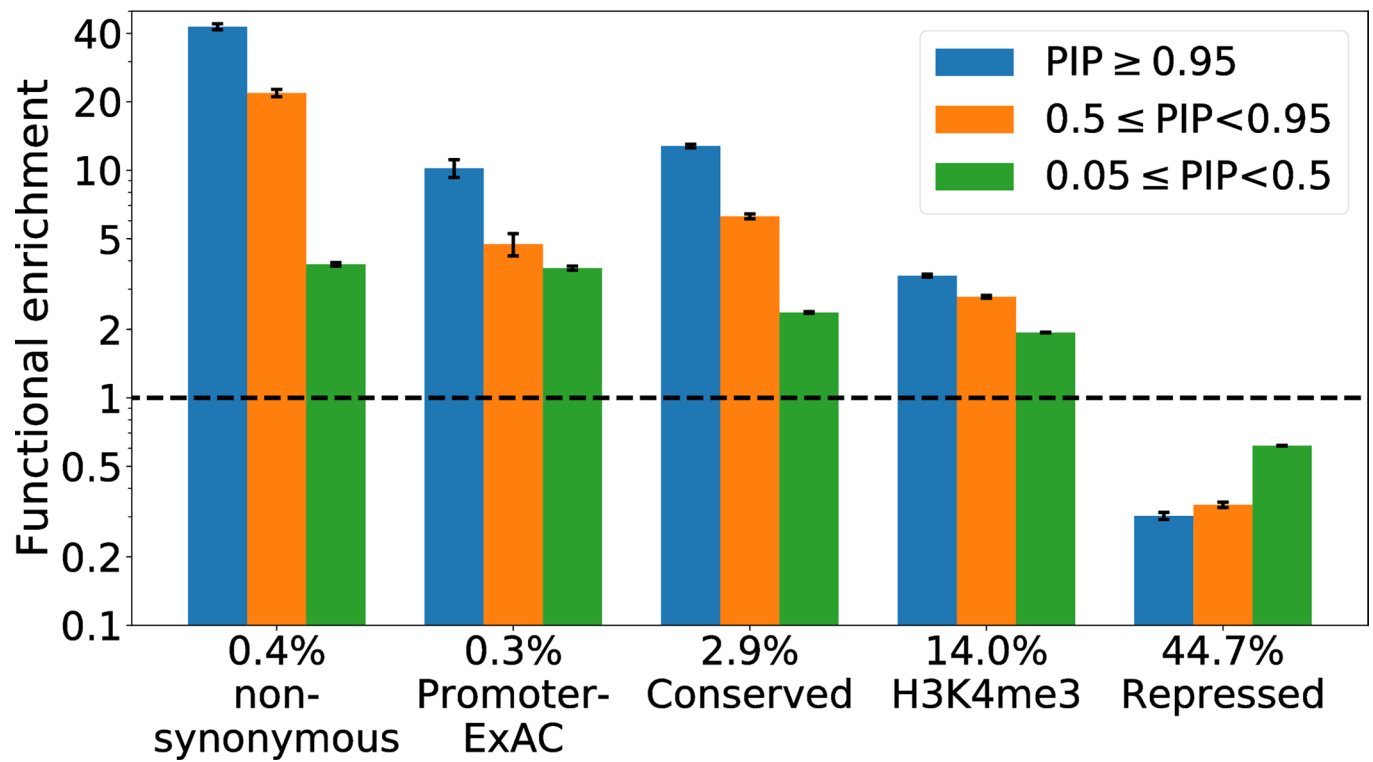
**Extended Data Fig. 5 | Assessing the individual impact of step 5 of PolyFun (specifying prior causal probabilities in proportion of the re-estimated per-SNP heritabilities) via perturbation analysis, by randomly permuting estimated prior causal probabilities.** The figure is similar to Extended Data Figure 1 but applies a different perturbation (randomly permuting estimated prior causal probabilities). Numerical reports are provided in Supplementary Table 6.



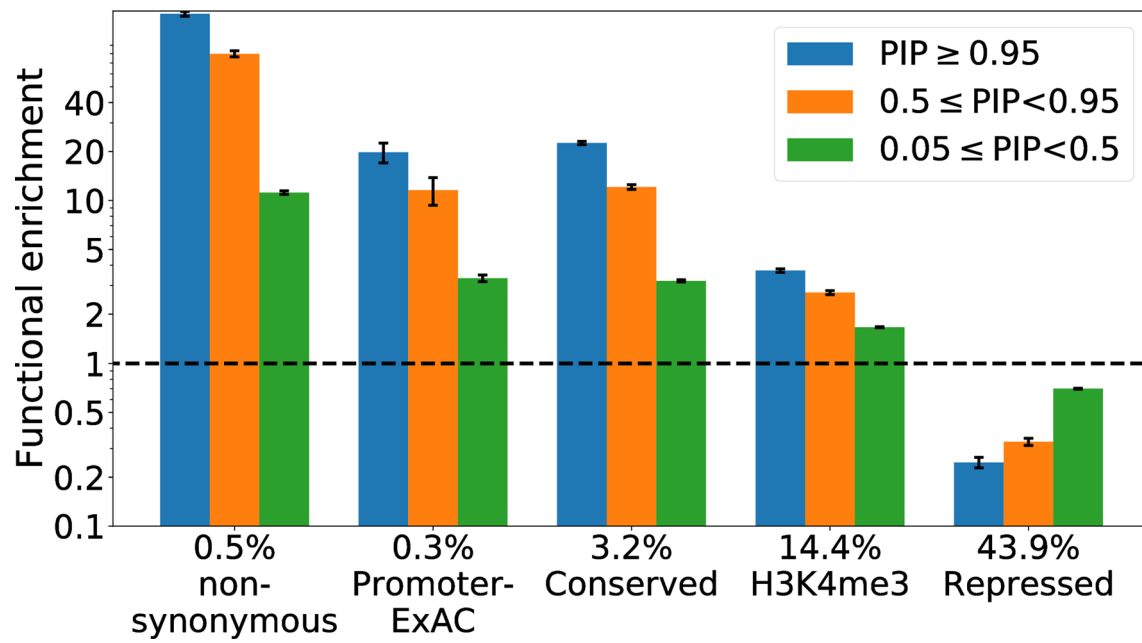
**Extended Data Fig. 6 | Visualization of fine-mapping results for UK Biobank traits.** We display an ideogram of all 2,225  $PIP > 0.95$  fine-mapped SNPs identified by PolyFun + SuSiE across 49 UK Biobank traits. Traits are color-coded into groups (see legend and Supplementary Table 8). White circles indicate SNPs that are pleiotropic for  $\geq 2$  genetically uncorrelated traits, with circles to the right of a white circle denoting the genetically uncorrelated traits (max of 5 colored circles due to space limitations). Numerical results are reported in Supplementary Table 10.



**Extended Data Fig. 7 | Functional enrichment of PolyFun + SuSiE fine-mapped common SNPs for UK Biobank traits.** The figure is analogous to Fig. 4 but uses PIPs computed by PolyFun + SuSiE instead of SuSiE. Numerical results are reported in Supplementary Table 26.



**Extended Data Fig. 8 | Functional enrichment of SuSiE fine-mapped  $\text{MAF} > 0.001$  SNPs for UK Biobank traits.** The figure is analogous to Fig. 4 but uses  $\text{MAF} > 0.001$  SNPs instead of common ( $\text{MAF} > 0.05$ ) SNPs. Numerical results are reported in Supplementary Table 27.



**Extended Data Fig. 9 | Functional enrichment of SuSiE fine-mapped low-frequency and rare SNPs for UK Biobank traits.** The figure is analogous to Fig. 4 but uses only low-frequency and rare SNPs ( $0.05 > \text{MAF} > 0.001$ ) instead of common ( $\text{MAF} > 0.05$ ) SNPs. Numerical results are reported in Supplementary Table 28.

## Reporting Summary

Nature Research wishes to improve the reproducibility of the work that we publish. This form provides structure for consistency and transparency in reporting. For further information on Nature Research policies, see [Authors & Referees](#) and the [Editorial Policy Checklist](#).

### Statistics

For all statistical analyses, confirm that the following items are present in the figure legend, table legend, main text, or Methods section.

n/a Confirmed

- The exact sample size ( $n$ ) for each experimental group/condition, given as a discrete number and unit of measurement
- A statement on whether measurements were taken from distinct samples or whether the same sample was measured repeatedly
- The statistical test(s) used AND whether they are one- or two-sided  
*Only common tests should be described solely by name; describe more complex techniques in the Methods section.*
- A description of all covariates tested
- A description of any assumptions or corrections, such as tests of normality and adjustment for multiple comparisons
- A full description of the statistical parameters including central tendency (e.g. means) or other basic estimates (e.g. regression coefficient) AND variation (e.g. standard deviation) or associated estimates of uncertainty (e.g. confidence intervals)
- For null hypothesis testing, the test statistic (e.g.  $F$ ,  $t$ ,  $r$ ) with confidence intervals, effect sizes, degrees of freedom and  $P$  value noted  
*Give  $P$  values as exact values whenever suitable.*
- For Bayesian analysis, information on the choice of priors and Markov chain Monte Carlo settings
- For hierarchical and complex designs, identification of the appropriate level for tests and full reporting of outcomes
- Estimates of effect sizes (e.g. Cohen's  $d$ , Pearson's  $r$ ), indicating how they were calculated

*Our web collection on [statistics for biologists](#) contains articles on many of the points above.*

### Software and code

Policy information about [availability of computer code](#)

Data collection

We did not collect data for this study. We analyzed raw genotype-phenotype data from UKBB (application 16549). Fine-mapping results generated in this study are available at [https://data.broadinstitute.org/alkesgroup/polyfun\\_results](https://data.broadinstitute.org/alkesgroup/polyfun_results)

Data analysis

Our PolyFun and PolyLoc software packages is available at <https://github.com/omerwe/polyfun>  
 Our baseline-LF model version 2.2 is available at [https://data.broadinstitute.org/alkesgroup/LDSCORE/baselineLF\\_v2.2.UKB.polyfun.tar.gz](https://data.broadinstitute.org/alkesgroup/LDSCORE/baselineLF_v2.2.UKB.polyfun.tar.gz)  
 Summary LD information analyzed in our study is available at [https://data.broadinstitute.org/alkesgroup/UKBB\\_LD](https://data.broadinstitute.org/alkesgroup/UKBB_LD)  
 Access to the UK Biobank resource is available via application (<http://www.ukbiobank.ac.uk/>)  
 SuSIE v0.7.1.0487 is available at <https://github.com/stephenslab/susieR>  
 FINEMAP v1.3.1 is available at <http://www.christianbenner.com>  
 PAINTOR v3.1 is available at [https://github.com/gkichaev/PAINTOR\\_V3.0](https://github.com/gkichaev/PAINTOR_V3.0)  
 CAVIARBF v0.2.1 is available at <https://bitbucket.org/Wenan/caviarbf>  
 BOLT-LMM v2.3.4 is available at <https://data.broadinstitute.org/alkesgroup/BOLT-LMM/>

For manuscripts utilizing custom algorithms or software that are central to the research but not yet described in published literature, software must be made available to editors/reviewers. We strongly encourage code deposition in a community repository (e.g. GitHub). See the Nature Research [guidelines for submitting code & software](#) for further information.

### Data

Policy information about [availability of data](#)

All manuscripts must include a [data availability statement](#). This statement should provide the following information, where applicable:

- Accession codes, unique identifiers, or web links for publicly available datasets
- A list of figures that have associated raw data
- A description of any restrictions on data availability

PolyFun fine-mapping results generated in this study are available for public download at [http://data.broadinstitute.org/alkesgroup/polyfun\\_results](http://data.broadinstitute.org/alkesgroup/polyfun_results). Summary LD information generated in this study is available for public download at [https://data.broadinstitute.org/alkesgroup/UKBB\\_LD](https://data.broadinstitute.org/alkesgroup/UKBB_LD). Baseline-LF v2.2.UKB annotations and

## Field-specific reporting

Please select the one below that is the best fit for your research. If you are not sure, read the appropriate sections before making your selection.

Life sciences       Behavioural & social sciences       Ecological, evolutionary & environmental sciences

For a reference copy of the document with all sections, see [nature.com/documents/nr-reporting-summary-flat.pdf](http://nature.com/documents/nr-reporting-summary-flat.pdf)

## Life sciences study design

All studies must disclose on these points even when the disclosure is negative.

Sample size	We used N=337K unrelated British-ancestry individuals in the UK Biobank (the largest suitable sample available to us) for fine-mapping. We used N=122K European-ancestry individuals that were not used for fine-mapping for polygenic localization.
Data exclusions	We excluded the MHC region from all analyses and analyzed only autosomes.
Replication	No replication dataset was analyzed as fine-mapping requires access to individual-level genotypic data from hundreds of thousands of individuals, which is generally not publicly available other than the UK Biobank.
Randomization	We performed no randomization and analyzed all European-ancestry individuals from UK Biobank.
Blinding	We did not collect data for this study, but analyzed data from UK Biobank.

## Reporting for specific materials, systems and methods

We require information from authors about some types of materials, experimental systems and methods used in many studies. Here, indicate whether each material, system or method listed is relevant to your study. If you are not sure if a list item applies to your research, read the appropriate section before selecting a response.

### Materials & experimental systems

n/a	Involved in the study
<input checked="" type="checkbox"/>	<input type="checkbox"/> Antibodies
<input checked="" type="checkbox"/>	<input type="checkbox"/> Eukaryotic cell lines
<input checked="" type="checkbox"/>	<input type="checkbox"/> Palaeontology
<input checked="" type="checkbox"/>	<input type="checkbox"/> Animals and other organisms
<input checked="" type="checkbox"/>	<input type="checkbox"/> Human research participants
<input checked="" type="checkbox"/>	<input type="checkbox"/> Clinical data

### Methods

n/a	Involved in the study
<input checked="" type="checkbox"/>	<input type="checkbox"/> ChIP-seq
<input checked="" type="checkbox"/>	<input type="checkbox"/> Flow cytometry
<input checked="" type="checkbox"/>	<input type="checkbox"/> MRI-based neuroimaging